The Formation of New England Coastal Fronts

JOHN W. NIELSEN

Center for Meteorology and Physical Oceanography, Massachusetts Institute of Technology, Cambridge, Massachusetts

(Manuscript received 12 July 1988, in final form 16 December 1988)

ABSTRACT

Coastal fronts are a frequent late fall and early winter feature of eastern New England weather. Data from a mesoscale observing network is used to describe the process of coastal frontogenesis and to determine the causes of formation. Three distinct types of coastal frontogenesis are found to occur in New England, and examples of each are presented using mesoscale surface maps and time series. Type A coastal fronts form during cold air outbreaks as winds veer from offshore to onshore. Type B coastal fronts form in the evening as air temperatures over land fall below air temperatures over water. Both types of fronts represent thermally direct circulations which are created by heating from the warm sea surface, often in combination with radiational cooling over land. Type C coastal fronts are caused by upstream blocking when a stable region of warm advection, such as warm front, approaches the Appalachian Mountains from the south.

Type A and Type B coastal fronts are described in terms of land and sea breeze dynamics. The persistent, quasi-stationary nature of such coastal fronts is investigated with a simple two-layer density current model. It is found that the effects on frontal motion of an increasing onshore wind and heating from the sea surface tend to cancel each other, resulting in fronts which tend to remain stationary just offshore.

1. Introduction

Bosart et al. (1972) used the term *coastal front* to refer to a late fall and early winter boundary layer feature common to the New England area. They described coastal fronts as forming locally near the coast and separating an easterly maritime airflow off the Atlantic from the cold northerly outflow of an anticyclone. They noted that coastal fronts often involve 10°C temperature contrasts over distances of 5 to 10 km and frequently mark the boundary between rain and freezing rain or snow. They identified surface friction, orography, coastal configuration, and land–sea thermal contrast as being important factors governing coastal frontogenesis.

Subsequent observations of New England coastal fronts have shown that the frontal temperature contrast can be as sharp as 5°C in 1 km (Sanders 1983). The fronts can be hundreds of kilometers long and typically persist for 6 to 48 hours prior to the passage of surface cyclones. The frontal inversion becomes level behind the surface front at an altitude of about 300 to 500 m above ground level (Neilley 1984). The cold air is isolated between the front and the adjacent Appalachian Mountains, and tends to be stagnant near the ground. Diagnostic calculations (e.g., Bosart et al. 1972) have consistently demonstrated that coastal frontogenesis occurs in the absence of background geostrophic frontogenesis.

Case studies of various New England coastal fronts are contained in Bosart et al. (1972), Bosart (1975), and Marks and Austin (1979). Bosart et al. identified the Carolina and south Texas coasts as additional favored locations for coastal frontogenesis within the United States, and examples of coastal fronts in those locations may be found in Bosart (1981) and Bosart (1984). Coastal frontogenesis also occurs in other parts of the world, such as the western edge of the Black Sea (Draghici 1984), the southern coast of Norway (Fig. 6 of Bergeron 1949), and the northwest coast of the Netherlands (Roeloffzen et al. 1986).

The critical mechanism for the onset of coastal frontogenesis in New England has been variously identified as differential friction (Bosart 1975), differential heating (Ballentine 1980), and upstream blocking by orography (Garner 1986). It is the purpose of this paper to distinguish between these competing mechanisms through the use of data from a mesoscale network in place during November and December 1983 for the New England Winter Storms Experiment (NEWSEX). Five-minute data are available from 15 Portable Automated Mesonet II (PAM) stations which had been installed across southeastern New England. Figure 1 shows the locations of the PAM stations, as well as hourly stations, coast guard stations, and upper air stations. Coupled with standard meteorological observations, the PAM data permits detailed description of the coastal frontogenetical process and determination of the governing mechanisms.

Corresponding author address: John W. Nielsen, Center for Meteorology and Physical Oceanography, Room 54-1814, Massachusetts Institute of Technology, Cambridge, MA 02139.

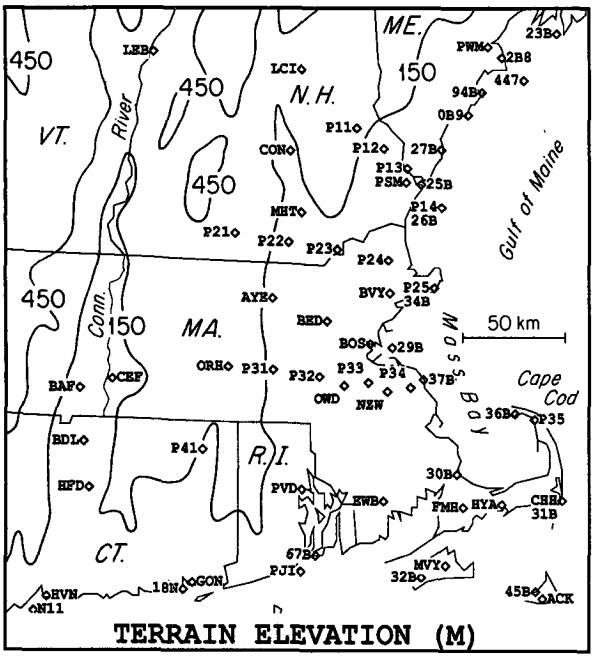

FIG. 1. Map of southeastern New England, showing contours of surface elevation (m) and locations of hourly, Coast Guard, and upper air stations and other places mentioned in the text. Stations whose identifiers consist of P followed by two digits are temporary PAM station sites. The PAM stations made observations at five-minute intervals during NEWSEX.

Also depicted in Fig. 1 is the orography of southern New England. Coastal plains give way to low mountains 50–100 km inland. The ridge crests vary in elevation from 250 to 600 m, with ridges of over 1000 m to the north and northwest beyond the domain of the map.

Three distinct types of coastal frontogenesis were observed during NEWSEX. The three types are defined in section 2, and the representativeness of the two-month sample of New England coastal fronts is discussed. In section 3, case studies for each type of frontogenesis are presented. Mesoscale surface maps and PAM station time series are used to examine the development of the fronts and the evolution of the horizontal frontal structure. In section 4, Type A and Type B coastal fronts are described by analogy to land and sea breeze circulations, and a density current model is developed to investigate the motion of such coastal fronts. Section 5 identifies Type C coastal fronts as manifestations of a form of orographically forced frontogenesis studied by Garner (1986). The principal results are discussed in section 6 with reference to coastal front forecasting and coastal frontogenesis in other areas.

2. Identification and categorization of coastal fronts observed during NEWSEX

Since, to our knowledge, the term coastal front has not been explicitly defined in the literature, we adopted a set of criteria to distinguish coastal fronts from other fronts or nonfrontal systems occurring during NEWSEX. We required first that there be a surface front; that is, two relatively homogeneous boundary layer air masses separated by a convergent boundary less than 10 km wide marked by localized gradients of wind and temperature. We required that the front be coherent and quasi-linear over a length of at least 100 km, with the front extending at least partly through the PAM network in eastern Massachusetts and southeastern New Hampshire. We required that the front form within 100 km of the coastline, remain in the vicinity of the coast through most of its lifetime, and be oriented roughly parallel to the coast with the warmer air being on the seaward side of the front. During NEWSEX (November and December 1983), 13 events satisfied the above criteria.

Bosart (1975) constructed a nine-year climatology of New England coastal fronts from three-hourly surface maps, by searching for wind and temperature differences between selected New England stations. Bosart found that three to four coastal fronts occur on average during November and December. While conditions during 1983 were generally favorable for coastal frontogenesis (the mean land–sea temperature contrast in east-central New England was 0.8°C greater than normal and precipitation was above normal[1]), much of the difference between the NEWSEX observations and the climatology is due to difficulties, recognized by Bosart, in identifying coastal fronts using 3-hourly synoptic maps. Applying Bosart's method to the November–December 1983 maps, we were able to identify only three of the 13 coastal fronts. It is therefore likely that the climatology of Bosart (1975) of 6.3 coastal fronts per year underestimates the frequency of New England coastal fronts by at least a factor of two.

Bosart (1975) also constructed a map of composite surface pressure for the time of onset of his 57 coastal front cases. The composite (Fig. 2) shows the synoptic features which have come to be associated with coastal fronts. The anticyclone northeast of New England is particularly well defined, while the mean cyclone to the southwest is comparatively broad and diffuse, a consequence of averaging over many cyclone locations. Also appearing in the composite is an inverted ridge of high pressure extending from southern New England through Maryland. This inverted ridge is symptomatic of cold-air damming (Forbes et al. 1987; Bell and Bosart 1988), which involves shallow cold air trapped to the east of the Appalachians.

[1] Data: NCDC Climatological Data Annual Summary, New England 1983; NWS/NESDIS Oceanographic Monthly Summary, November and December 1983 (U.S. Dept. of Commerce, Washington, D.C.). The land–sea contrast was calculated from sea surface temperature anomalies averaged over the region 42°–45°N, 66°–71°W and average departures from normal of five climatological zones in Maine, New Hampshire, and Massachusetts.

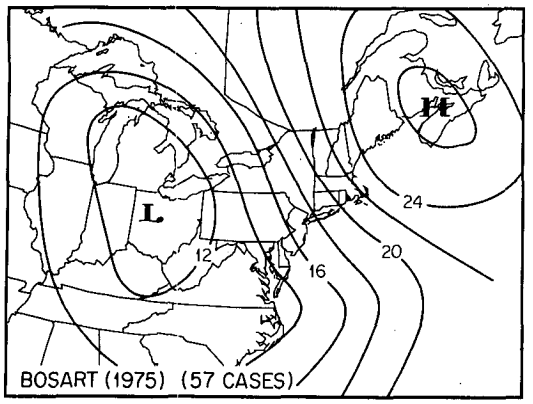

FIG. 2. Composite surface pressure at time of onset of 57 cases of New England coastal frontogenesis between 1964 and 1972, redrawn from Bosart (1975). Contour interval is 2 mb.

To verify the representativeness of the NEWSEX sample, analogous composites were constructed for the 13 NEWSEX cases, using synoptic maps nearest the times 3 hours before and 3 hours after front formation. The pressure analyses were reduced to two degree latitude–longitude grids and averaged. The resulting composites (Fig. 3) are indeed similar to the Bosart composite. The best match is found with the composite of pressure 3 hours after front formation. Although there is no closed anticyclone, the broad ridge of high pressure in Fig. 3b is colocated with the anticyclone of Fig. 2. Both maps show the lowest pressures in the Midwest, a trough extending into the western Atlantic, and an inverted ridge along the mid-Atlantic states. The geostrophic wind direction, speed, and curvature in the region of coastal frontogenesis along the New England coast appear to be nearly identical.

Bosart (1975) has classified New England coastal fronts according to five synoptic categories representing the general synoptic situation at the time of frontogenesis. As nearly all New England coastal front situations share the common characteristic of high pressure northeast of New England, the synoptic categories were defined by the track and intensity of the advancing cyclones. However, New England coastal frontogenesis often bears little relationship to the characteristics of approaching cyclones. Instead, as will be shown below, the nature of the coastal frontogenesis is strongly dependent on the local wind and temperature patterns. We therefore abandon Bosart's classification system in favor of a classification based on differences in the timing and location of coastal frontogenesis in New England. We designate the three observed classes of coastal frontogenesis as Types A, B, and C. The three types are briefly identified below, with detailed descriptions deferred to section 3.

Type A coastal frontogenesis was the most common type among the 13 cases observed. It takes place during the transition from offshore winds to onshore winds caused by the passage of a ridge of high pressure from west to east. Inland winds fail to shift, and a convergence zone is rapidly established along the coast.

Type B coastal frontogenesis is triggered not by a passing ridge but by nightfall. Prior to frontogenesis, winds are onshore and light. As the land–sea thermal contrast increases diurnally, inland winds back and become northerly, again establishing a convergence zone along the coast.

Type C coastal frontogenesis occurs in a relatively warm environment characterized by moderate onshore winds. The coastal front forms a few tens of kilometers inland, roughly halfway between the coast and the low inland mountains.

The 13 coastal fronts observed within the PAM network during NEWSEX are classified by type in Table 1.

3. Examples of three types of New England coastal frontogenesis

a. An example of Type A coastal frontogenesis

During the early hours of 4 December 1983, a broad anticyclone moved slowly eastward across northern

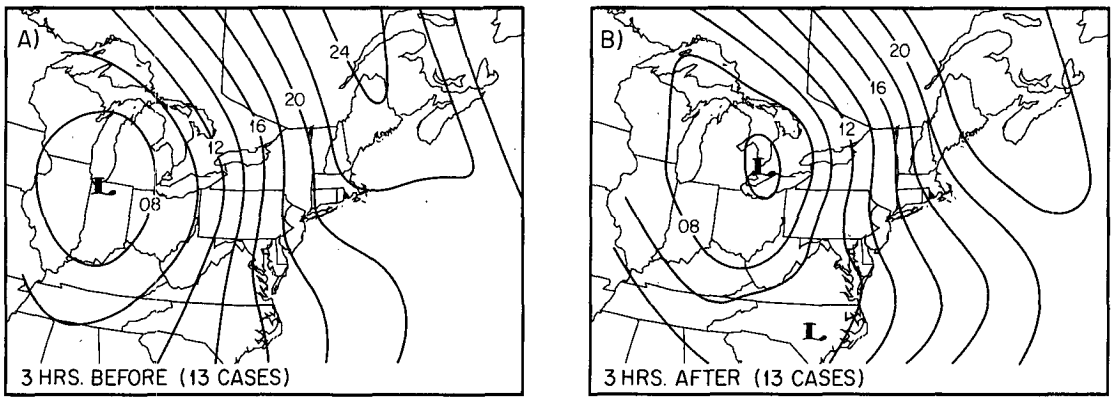

FIG. 3. Composite surface pressure analyses for 13 NEWSEX coastal front cases. Contour interval is 2 mb. (a) Three hours before coastal front formation. (b) Three hours after coastal front formation.

TABLE 1. New England coastal fronts observed during Nov–Dec 1983 (Time UTC).

Time of formation	Time of extinction	Type
0000 10 Nov	1300 10 Nov	A
0300 14 Nov	1500 14 Nov	A
0100 15 Nov	1700 15 Nov	B
1200 16 Nov	2200 16 Nov	C
2200 20 Nov	1300 21 Nov	C
0000 25 Nov	1200 25 Nov	C
2300 28 Nov	1200 29 Nov	B
0500 4 Dec	1000 5 Dec	A
1000 6 Dec	1800 6 Dec	A
2300 6 Dec	0600 7 Dec	C
0000 12 Dec	1000 13 Dec	B
0500 22 Dec	2300 22 Dec	A
1300 28 Dec	0300 29 Dec	A

New England (Fig. 4). A weak cyclone traveled up the Ohio Valley, with secondary development occurring along a warm front in the Carolinas. This overall weather pattern was identified by Bosart et al. (1972) as being typical of coastal frontogenesis situations, and indeed a Type A coastal front formed. Note that the frontal system associated with the cyclone remained well to the south and west, and that the geostrophic flow along the New England coast remained anticyclonic.

The pressure pattern, winds, and temperatures in southern New England during coastal frontogenesis are shown in Fig. 5. The sea level pressure has been analyzed subjectively from pressure observations which have been corrected for systematic errors. Wind speeds are plotted with a nonstandard convention: a long barb equals 1 m s^{-1} and a pennant equals 5 m s^{-1}. Coastal fronts are depicted using the standard meteorological symbol for stationary fronts, with a dashed line used in ambiguous regions. The analysis of the coastal fronts is based primarily on time series at individual stations.

Even before the coastal front formed (Fig. 5a), conditions along the coast and offshore differed from conditions inland. Winds were stronger, and heating by the 6°–8°C sea surface was helping to produce an east–west temperature gradient.[2] However, the wind was still divergent along the coast. During the following 9 hours (Figs. 5b–d), the offshore winds veered and strengthened, responding to the motion of the anticyclone from west to east. Coastal temperatures rose slightly, as winds carried air parcels farther out over the warm Gulf of Maine. Inland, winds had become more coherent from station to station. They never developed an onshore component, and instead blew parallel to the coast and the mountains.

[2] Sea surface temperature measurements are from offshore buoys and from Coast Guard stations along the Gulf of Maine coast.

The coastal front had begun to form as soon as winds over water developed an onshore component. The front was initially about 20 km offshore, but it immediately began drifting onshore at a speed of 1–3 m s^{-1}. Once the confluence was established, the temperature difference across the front grew rapidly as the front became a boundary between air which had been cooled radiationally over land and air being heated by the Gulf of Maine. Overcast skies after 0600 UTC inhibited further cooling. Trajectory analyses of parcels leaving the Maine coast and reaching the vicinity of the coastal front between 0600 and 1200 UTC suggest overwater temperature increases of 3°–5°C.

Time series from the middle and southern rows of PAM stations (Figs. 6 and 7) show the evolution of the frontal zone. Along with temperature, the wind component toward 115 deg (orthogonal to the coastal front) is plotted. Station P35 is included in both sets of time series and is representative of offshore conditions east of the coastal front, where the southeasterly component of the wind steadily increased between 0000 and 1400 UTC. The temperature at P35 was nearly constant at 1° to 2°C, the result of a rough balance between two competing effects: cold advection from the north and notheast, and diabatic heating from the sea surface along lengthening overwater trajectories.

The first coastal front passage in the PAM network was at station P25 (Fig. 6). The wind at P25 veered in tandem with the wind at P35 until about 0430 UTC, at which time the wind direction (not shown) became steady from the north-northwest. Starting at 0645 UTC, the wind veered rapidly and after 50 minutes was again similar to that at P35. The component of wind normal to the coastline changed from offshore at 3 m s^{-1} to onshore at 2 m s^{-1}, and the temperature increased by 1.5°C. This frontal passage was relatively weak and gradual because the front was only two to three hours old and moving slowly, and because air on the cold side of the front was being heated as it passed over the Gulf of Maine before reaching P25 (see Fig. 5b).

The next PAM frontal passage occurred at P34 (Fig. 7) between 0910 and 0940 UTC. The temperature increase was almost 4°C, much larger than at P25 because of nocturnal cooling at P34 prior to the frontal passage. As at P25, the wind shift and temperature jump occur simultaneously, and winds and temperatures rapidly become similar to those offshore at P35. The anomalous rise in temperature commencing at 0700 UTC was apparently due to a period of wind blowing southward from Massachusetts Bay.

The coastal front later passed stations P24 (Fig. 6) and P33 (Fig. 7) at nearly the same time. In both cases, the temperature rose 3.5°C, and winds changed from nearly calm to onshore. However, the passage at P33 took considerably longer. Observations from adjacent hourly stations (not shown) indicate that the front was becoming broad and diffuse in its southern portion. Hourly reports at PVD showed no sign of a frontal

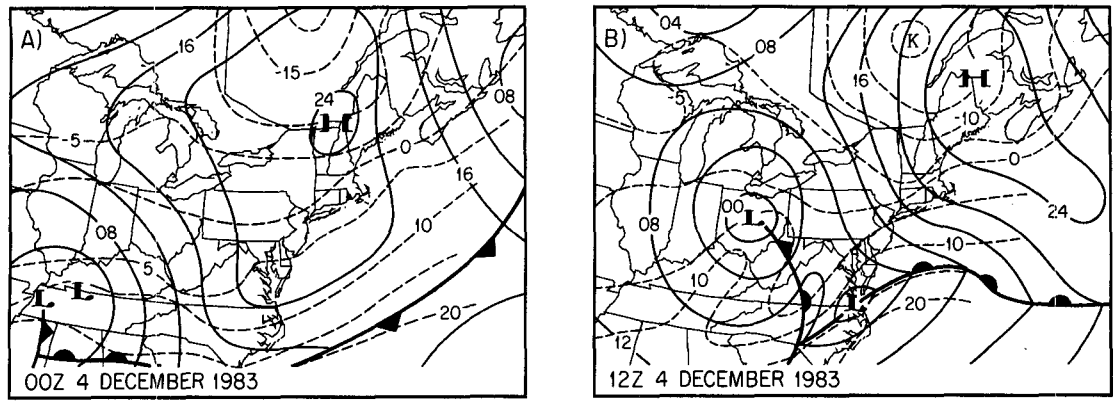

FIG. 4. Synoptic surface analyses of pressure (solid lines, contour interval 4 mb) and temperature (dashed lines, contour interval 5°C) before and after case of Type A coastal frontogenesis. Surface pressure and fronts are taken from NMC analyses; temperature was analyzed subjectively to show large-scale thermal structure. (a) 0000 UTC and (b) 1200 UTC 4 Dec 1983.

passage during the morning. Rough estimates of the width of the frontal zone, based on assumed constant frontal speeds between adjacent PAM stations, are 2.4 km at P24 and 7.8 km at P33. Direct observations of the frontal width by aircraft three hours later are consistent with these estimates. By comparison, Sanders (1983), using an instrumented automobile to penetrate a more intense front, found a frontal zone only a few hundred meters wide.

The coastal front described above is typical of the six coastal fronts during NEWSEX which formed along the coast as the winds became onshore. These Type A coastal fronts share the following characteristics:

- Air temperatures before frontogenesis are colder than sea surface temperatures.
- The coastal front forms quickly, within three hours, as easterly winds develop offshore.
- Winds inland do not veer to easterly, but instead become parallel to the coastal front and the mountains during the first few hours of frontogenesis.
- The temperature difference across the front is caused by the confluence of air parcels which have experienced differential heating.
- The fronts, which form locally along the coastline, are generally strongest in the vicinity of New Hampshire and tend to move slowly inland after forming.

Surface pressure composites of the six Type A coastal front cases (Fig. 8) depict the essential triggering mechanism of such frontogenesis: the veering of the wind along the coastline. Three hours prior to frontogenesis (Fig. 8a) the composite geostrophic wind is weakly offshore along the New England coast north of Boston. After frontogenesis (Fig. 8b) it is weakly onshore, a reversal seen not only in the composite but in each of the six individual cases from which it was constructed. The change is brought about by the motion of the anticyclone. Because this change in wind direction is not a characteristic of the other two types of New England coastal frontogenesis, it is not seen in the overall composite maps (Fig. 3).

A second characteristic of Type A frontogenesis, relatively cold air over land, produces a difference in the apparent strength of cold-air damming between Figs. 3 and 8. The inverted ridge, which stretches from Massachusetts into North Carolina, is more prominent in the Type A composite.

b. An example of Type B coastal frontogenesis

The Type B coastal frontogenesis of 15 November 1983 occurred one day after a case of Type A frontogenesis. The Type A front (not shown) formed at about 0500 UTC 14 November 1983 in a manner similar to the front of 4 December 1983. The principal differences are that in this case, the front remained mostly offshore, the anticyclone became stationary to the north so that winds over water did not veer beyond east-northeasterly, and the frontal temperature contrast was not as great. The latter difference led to dissipation of the coastal front in situ the next morning, at about 1500 UTC 14 November 1983, when air temperatures over land rose diurnally and became comparable to temperatures over water.

During the period of Type B frontogenesis, the anticyclone was located over New Brunswick (Fig. 9), and geostrophic winds along the New England coast were easterly throughout the period. A weak cyclone moved eastward off Cape Hatteras, and two other low centers were passing through the Midwest. Again, note the lack of frontal systems in the vicinity of New England.

Skies were overcast, and winds and temperatures varied little during the afternoon. The mesoscale analysis for 2100 UTC (1600 LST) 14 November 1983 (Fig. 10a) shows conditions which had prevailed for

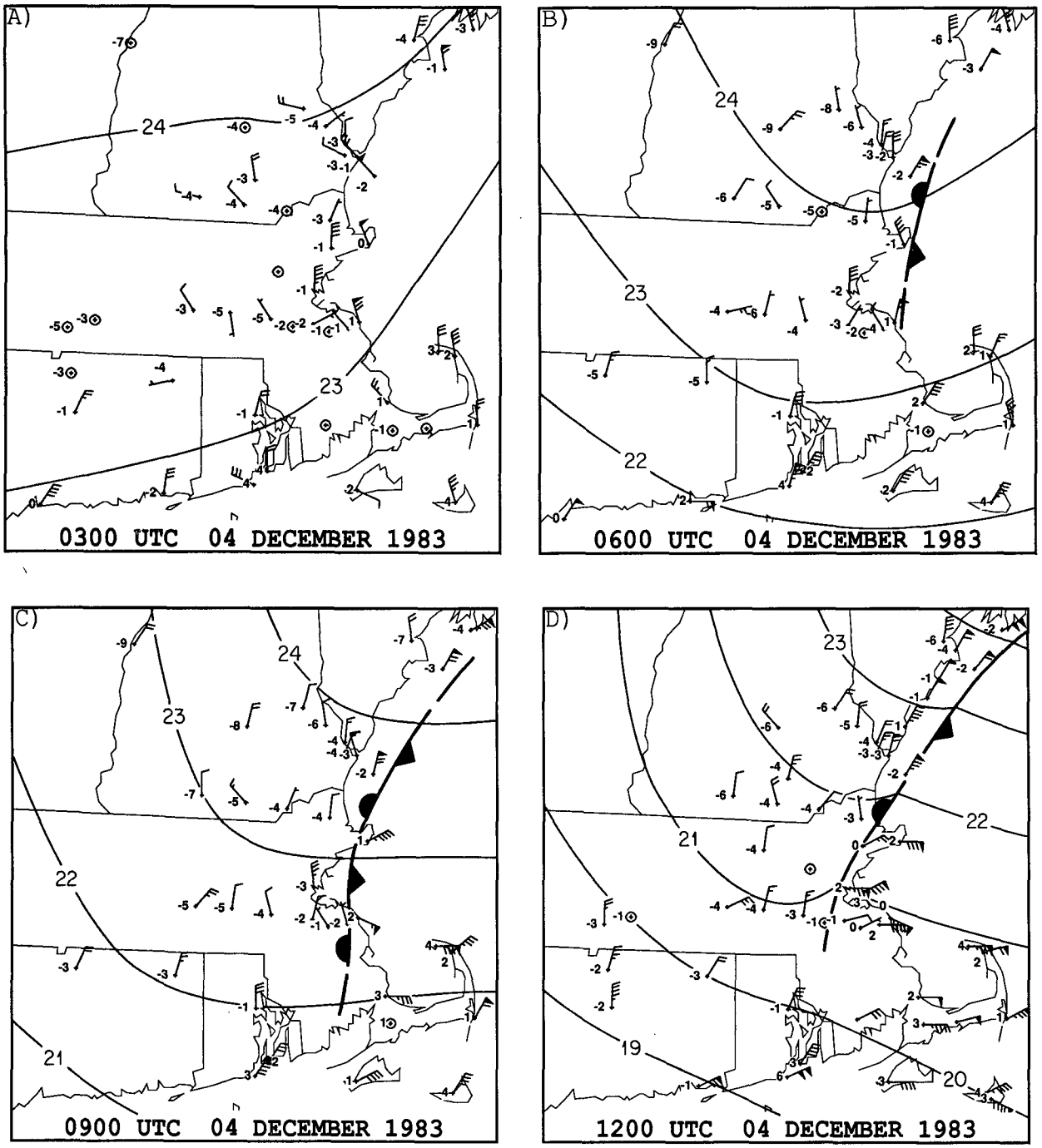

FIG. 5. Mesoscale surface analyses of Type A coastal frontogenesis, 4 Dec 1983. Pressure is analyzed subjectively with a 1 mb contour interval, and station values of temperature are plotted in degrees C. A single wind barb equals 1 m s^{-1}, a pennant equals 5 m s^{-1}. (a) 0300 UTC. (b) 0600 UTC. (c) 0900 UTC. (d) 1200 UTC.

3–5 hours. With weak cold advection present, the Gulf of Maine sea surface temperatures of 10°C were 3°–7°C warmer than air temperatures. Weak confluence, presumably frictionally induced, is present along the coastline. During early evening, 3 hours later (Fig. 10b), temperatures over land had already fallen diurnally by 1° to 2°C. Winds at most inland stations had weakened and backed, and were blowing parallel to the coast and the mountains, while winds offshore (for example, at 26B and 36B) remained northeasterly at

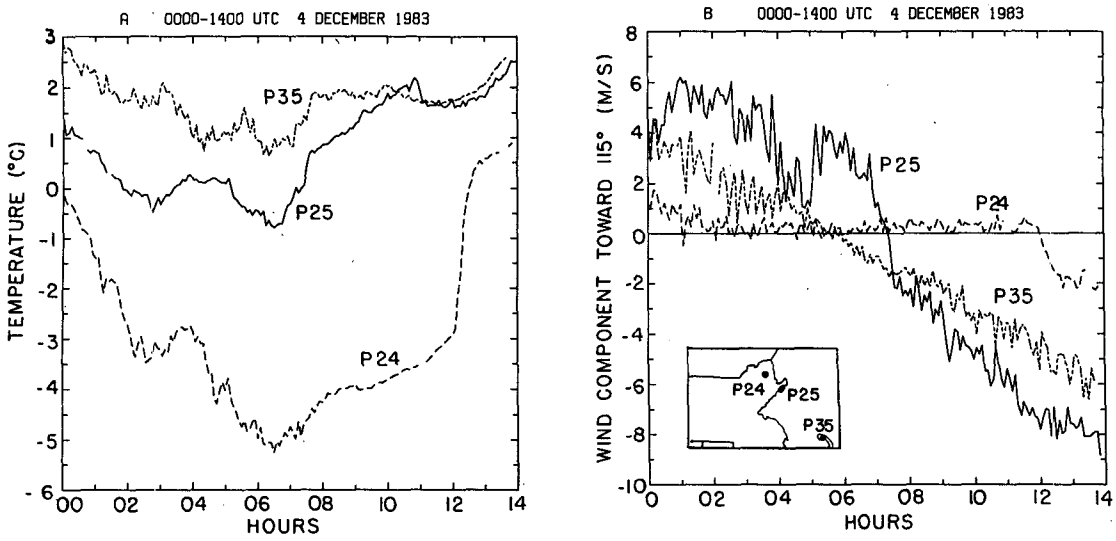

FIG. 6. Time series of (a) temperature (°C) and (b) front-normal wind speed (m s^{-1}) for PAM stations P24, P25, and P35, 0000 to 1400 UTC 4 Dec 1983. Inset shows locations of stations.

5–10 m s^{-1}. Both differential diabatic heating and coastal confluence were contributing to intensification of the temperature gradient along the coastline.

The wind at P25, along the northern Massachusetts coast, had also backed, suggesting a confluence zone developing to its east. Between 0100 and 0200 UTC the wind at P25 returned to east-northeasterly, with a concurrent temperature rise of 0.6°C. It is possible that these observations show the incipient coastal front moving westward past P25.

By 0300 UTC 15 November 1983 (Fig. 10c), a coastal front had formed along the coastline from Maine to Massachusetts. Winds over land had backed further and near the coast had developed a component toward the coastal front. Temperatures had fallen another 1°C over land but had remained steady over water, with half the overall temperature difference concentrated at the front. The front continued to intensify in place as inland temperatures continued to fall. At 0600 (Fig. 10d), the frontal temperature difference was 2° to 4°C, while the wind pattern had undergone little further evolution.

The evolution of the winds and temperatures on either side of the Type B coastal front can be seen with the time series in Fig. 11. The coastal station P34 had a wind off the water through most of the afternoon and

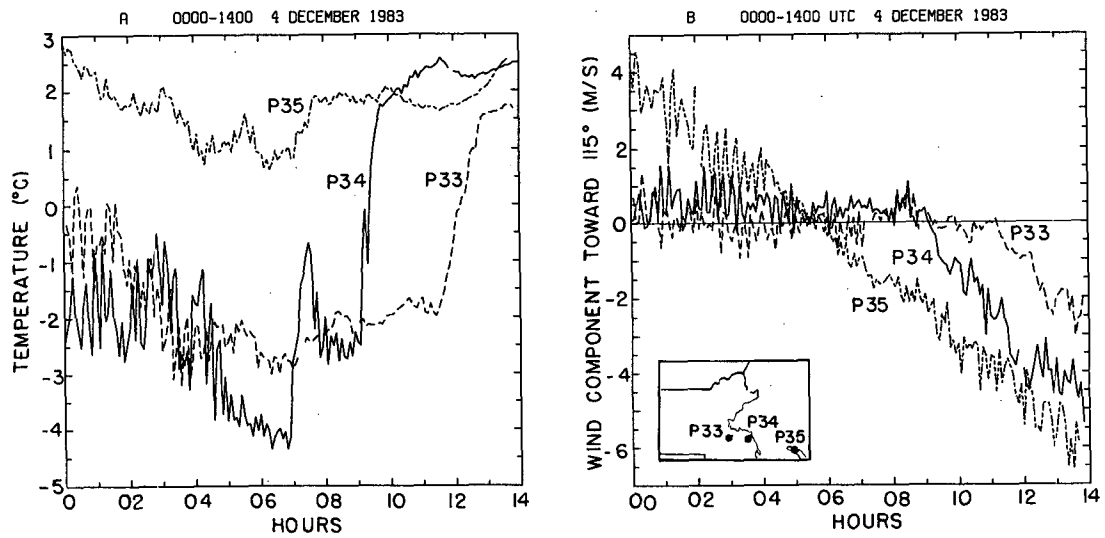

FIG. 7. As in Fig. 6, but for PAM stations P33, P34, and P35.

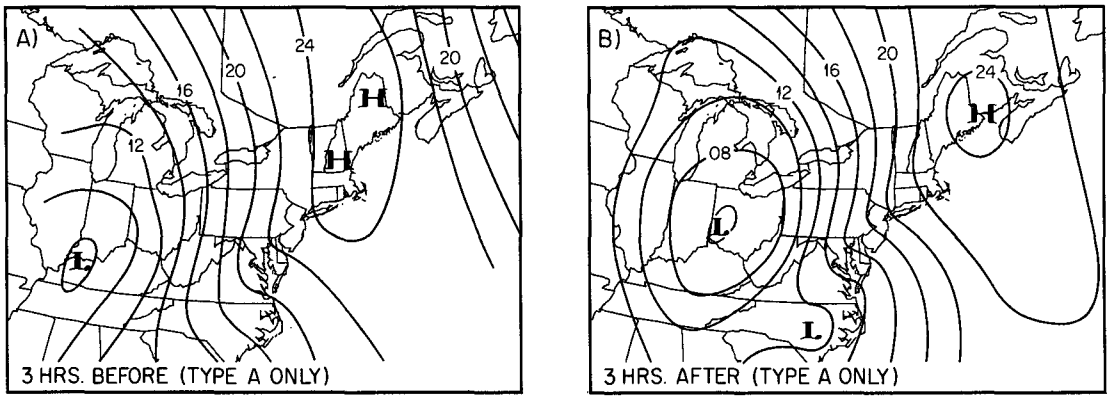

FIG. 8. Composite surface pressure analyses, as in Fig. 3, but for 6 Type A coastal front cases only.

evening, and its temperature varied little. The temperature at inland station P22 began falling early in the afternoon, finally reaching 0.8°C at 0300 UTC 15 November 1983. As the temperature fell, particularly in the evening, the wind backed and the front-normal wind component changed sign. By 0300 UTC, the coastal front had formed.

Between 0300 and 0730 UTC, the wind normal to the front at P34 gradually weakened. Finally, at 0745 UTC, the coastal front moved seaward past P34. The station, over a 15 minute period, experienced a change in front-normal wind of 2.5 m s^{-1} and a drop in temperature of 2.3°C. Three hours later, the coastal front had reversed direction and again passed P34, this time heading inland. The temperature rose 2.2°C, and the wind change, a bit less distinct, was about 1.5 m s^{-1}. In the context of density current theory to be discussed later, this reversal of frontal motion may be attributed to an observed decrease in frontal temperature contrast of 0.7°C and an increase in onshore wind speed of 0.7 m s^{-1} between 0745 and 1045 UTC.

There were three Type B coastal fronts during the two months of NEWSEX. They share the following common features:

- Initially, temperatures over the coastal plain are comparable to temperatures over water and the wind is weakly onshore. The component of wind normal to the coast in the three NEWSEX cases was 5 m s^{-1} or less.
- During the early evening, radiational cooling establishes a coastal temperature gradient. As the gradient develops, winds over land back until they are northerly. The backing often begins near the coast and spreads inland.
- The coastal front forms in the early evening within the coastal confluence zone.
- Once formed, the front and associated circulation patterns resemble those resulting from Type A coastal frontogenesis.

The pressure composites of the three Type B coastal frontogenesis events of NEWSEX (Fig. 12) are broadly

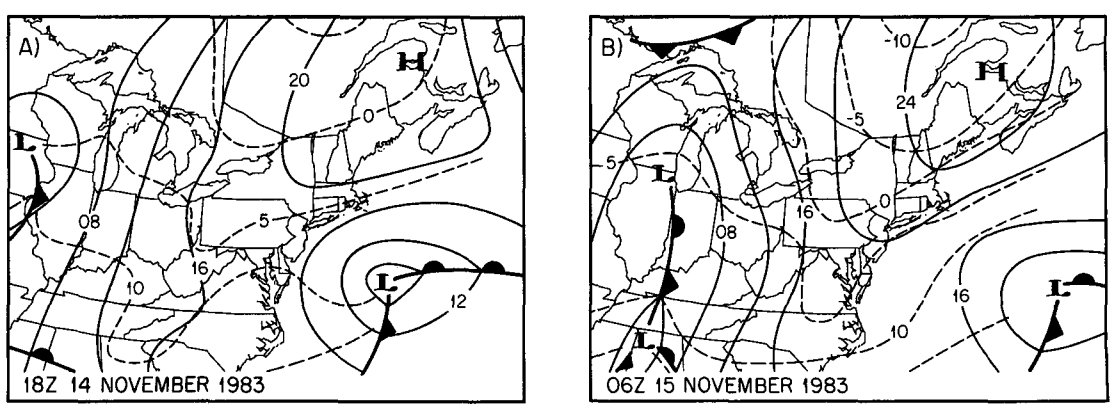

FIG. 9. Synoptic analyses (as in Fig. 4) before and after case of Type B coastal frontogenesis. (a) 1800 UTC 14 Nov 1983. (b) 0600 UTC 15 Nov 1983.

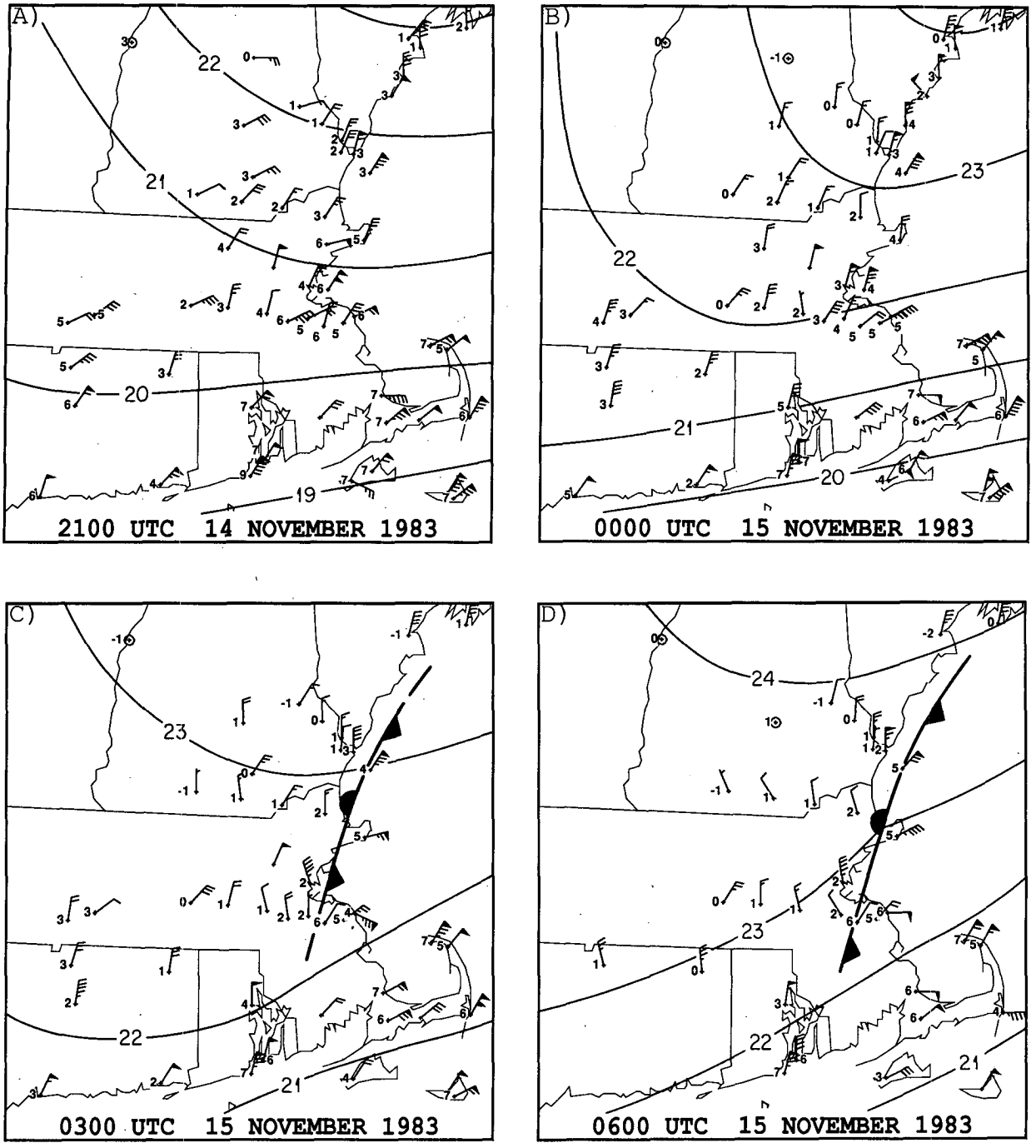

FIG. 10. Mesoscale analyses (as in Fig. 5) of Type B coastal frontogenesis, 14–15 Nov 1983. (a) 2100 UTC 14 Nov (b) 0000 UTC 15 Nov (c) 0300 UTC 15 Nov (d) 0600 UTC 15 Nov.

similar to the Type A composites (Fig. 8). Disregarding small-scale variations caused by the small number of Type B cases, the overall picture is of a situation several hours beyond that depicted in the Type A composites. Winds are onshore both before and after frontogenesis, and the anticyclone is moving eastward in the vicinity of the Canadian Maritimes. Cold-air damming appears much weaker in the Type B composite.

After the coastal front has formed and the inland northerly winds have become established, Type A and Type B fronts have no essential differences. This may be seen in a comparison of Figs. 5c and 10d. The an-

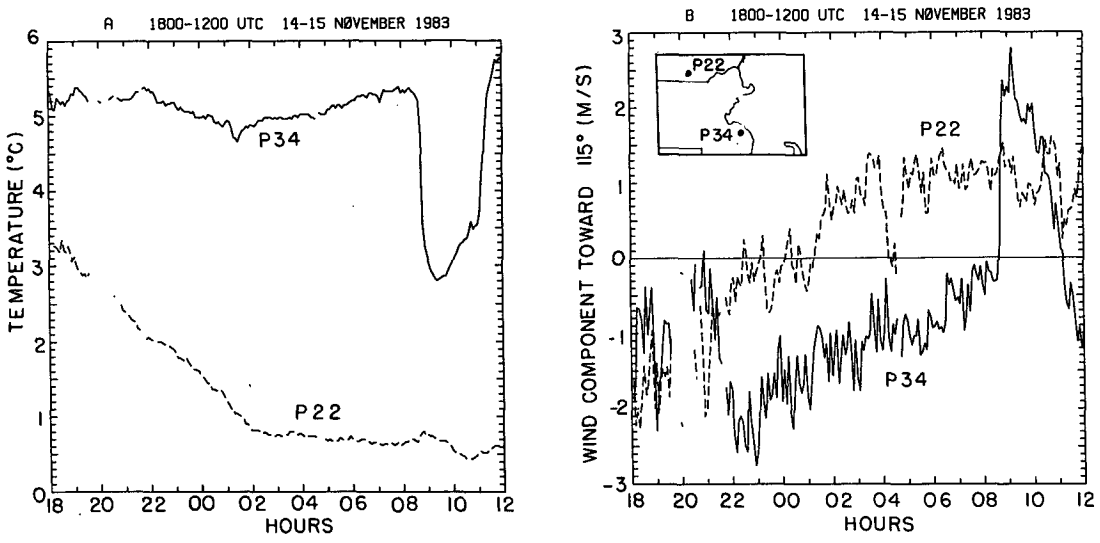

FIG. 11. Time series of (a) temperature and (b) front-normal wind speed (as in Fig. 6) for PAM stations P22 and P34, 1800 UTC 14 Nov 1983 to 1200 UTC 15 Nov 1983.

alyzed coastal fronts are nearly colocated. The winds on the warm wide of the front are similar, although this is due to the similarity in the large-scale pressure pattern rather than any influence of the coastal front. More significantly, the winds on the cold side of the coastal front, although nongeostrophic, are nearly identical. The Type A coastal front which fomed at 0300 UTC 14 November had even stronger similarities with this Type B case. With neither the large-scale pressure pattern nor the land–sea temperature difference varying between the two cases, the fronts formed in the same location (to the limit of the horizontal resolution of the stations), and the cold-air wind patterns were indistinguishable. The primary difference is simply in the sequence of events leading to formation: Type A fronts are triggered by the onset of onshore winds over water, while Type B fronts are triggered by diurnal cooling over land.

c. *An example of Type C coastal frontogenesis*

The most intense Type C coastal frontogenesis event during NEWSEX took place on 24–25 November 1983. During this frontogenesis event, large-scale winds were generally southerly in New England (Fig. 13). A deep, occluded cyclone was located in southern Canada, and an associated cold front stretched the length of the East Coast. Warm advection preceded the front along the Eastern Seaboard. The front moved offshore of the mid-Atlantic states after 0600 UTC 25 November 1983, and cyclogenesis followed. The cold front eventually reached eastern New England at 1200 UTC.

Throughout the period of frontogenesis, winds were generally southerly in southeastern New England (Fig. 14). Initially, exceptions were localized: a short-lived land breeze along the Maine coast, and drainage winds blowing down the Connecticut River valley. Beginning

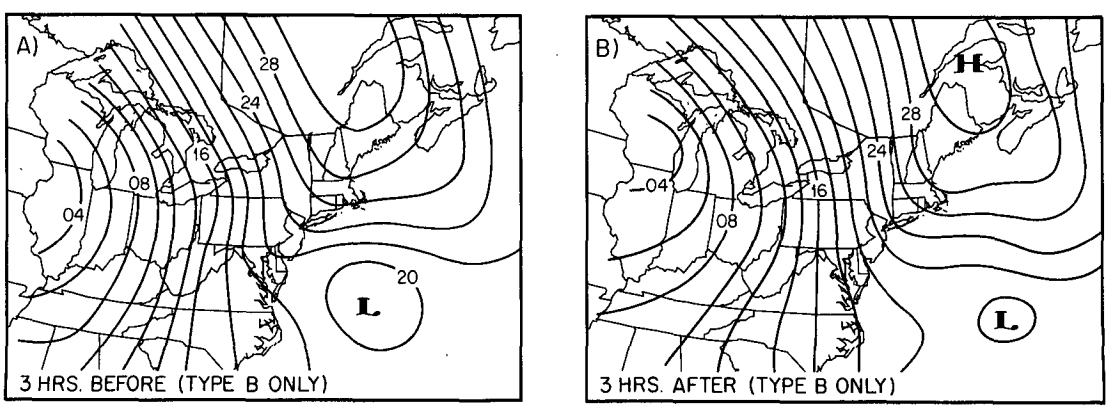

FIG. 12. Composite surface pressure analyses, as in Fig. 3, but for 3 Type B coastal front cases only.

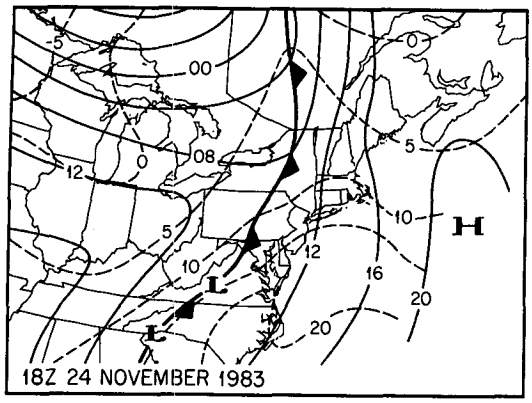

FIG. 13. Synoptic analysis (as in Fig. 4) before case of Type C coastal frontogenesis, 1800 UTC 24 Nov 1983.

at 2100 UTC 24 November 1983 (Fig. 14b), however, winds at many inland locations lost their southerly component. At about the same time, warmer air began reaching the area from the south, and temperatures at stations in the southerly airflow rose through the evening. The coastal front formed slowly. Unlike the previous two cases, it formed well inland from the coast, and a clear propagation of frontogenesis from south to north could be seen in time series of PAM stations spanning the frontal zone. Worcester, Massachusetts (ORH) remained in the warm air, even though the surface front was to the south. ORH is located near the southern end of a 300 m ridge, and the frontal inversion was below that level.

The primary differences between this situation and the situation during the Type B frontogenesis of 15 November 1983 (Fig. 10) are that the ambient wind direction is from the south rather than the east-northeast, and air temperatures over land are warmer, not slightly colder, than sea surface temperatures (8°C). Throughout this and other Type C coastal frontogenesis cases, differential diabatic heating across the coast contributes negatively to frontogenesis. The large temperature difference across the front (up to 7°C) was due entirely to strong warm advection on the warm side of the front. Temperatures on the cold side of the front remained relatively constant.

The evolution of the Type C front can be seen in Fig. 15, which shows time series from two stations located 23 km apart. Initially, both stations had southeast winds of 2 m s^{-1} and temperatures of 9°C, but warm advection began in earnest at station P32 at 2245 UTC. Soon, the wind component at P31 normal to the front (here taken to be positive toward 130 deg) changed sign and the temperature dropped 0.25°C. This appears to have been the type C coastal front in its earliest stage of formation. From that time on, the front developed in situ between the two stations. The temperature rose 5°C in 4 hours at P32, while remaining steady at P31. By 0700 UTC, the difference in temperature between these two stations was 7°C. The front eventually moved eastward, and at 1010 UTC the front passed P32, causing the temperature there to drop 3.9°C in 15 minutes.

The four cases of Type C coastal frontogenesis during NEWSEX share the following characteristics:

- Air temperatures are comparable to or warmer than sea surface temperatures.
- Large-scale warm advection from the south or southeast is occurring, often accompanied by radiational cooling at the surface.
- The front tends to form inland, near the base of the mountains.
- The first manifestation of coastal frontogenesis is a sudden decrease of wind speed or reversal of wind direction at inland stations.
- The temperature difference across the front is generated by warm advection within the warmer air.

The Type C pressure composites (Fig. 16) are markedly different from composites of the other two frontogenesis types. The composites are dominated by the presence of a large cyclone over the eastern Great Lakes. Winds along the New England coast are strongly onshore both before and after frontogenesis. The composite pressure pattern includes troughs suggestive of cold and warm fronts. As will be seen in section 5, the important feature of these composite maps is the warm frontal trough, which moves from roughly 39° to 41°N between the two composites.

4. Causes of Type A and B coastal fronts

a. A comparison of external factors governing coastal fronts and land–sea breezes

In all Type A and Type B frontogenesis cases during NEWSEX, air was being heated over water and cooled over land. Robust direct circulations also develop under similar circumstances during cold air outbreaks over Lake Michigan (Passarelli and Braham 1981; Ballentine 1982). These circulations have the sense of land breezes, but possess many of the characteristics of sea breezes.

Sea breezes tend to be stronger than land breezes, and numerical simulations also indicate an increased tendency for sea breezes to form fronts (Neumann and Mahrer 1971; Gross 1986). The relative weakness of the land breezes is usually attributed to the sign of the heating and the attendant differences in static stability (e.g., Defant 1951). Linear models indicate that the strength of the horizontal wind is inversely proportional to the stability (Niino 1987; Rotunno 1983). Increased stratification also inhibits the vertical transfer of heat and increases the effect of friction in slowing the circulation (Mak and Walsh 1976).

The presence of offshore heating during coastal frontogenesis leads to an environmental stratification characteristic more of sea breezes than of land breezes. Even in the three Type B cases, which were triggered

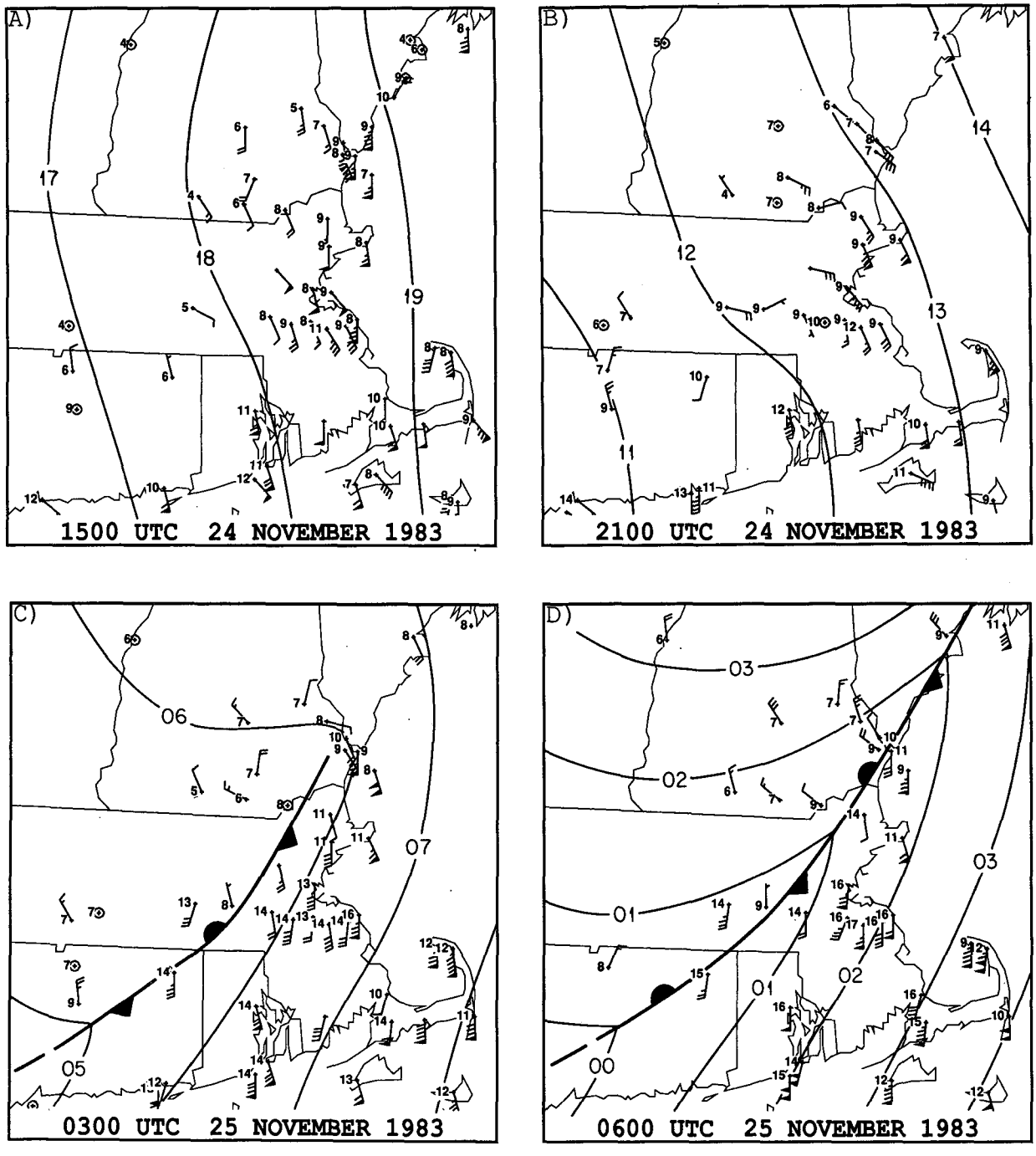

FIG. 14. Mesoscale analyses of Type C coastal frontogenesis, 24–25 Nov 1983. Plotting conventions as in Fig. 5. (a) 1500 UTC 24 Nov (b) 2100 UTC 24 Nov (c) 0300 UTC 25 Nov (d) 0600 UTC 25 Nov.

by cooling over land, the mean 0000 UTC stability, $[(g/\theta_0)\delta\theta/\delta z]^{1/2}$, through the lowest 50 mb at the upper air sites in Portland, Maine (PWM) and Chatham, Massachusetts (CHH) averaged just 0.6×10^{-2} s^{-1}, with a range from 0.0×10^{-2} to 1.2×10^{-2} s^{-1}.

The magnitude of the thermal forcing associated with Type A and Type B frontogenesis is easily as strong as that associated with ordinary sea breezes. Sea breezes can form under light offshore wind conditions when the temperature difference is as small as 1°–3°C (Watts 1955). In southern New England, individual case studies of the vertical structure of sea breezes (Craig et

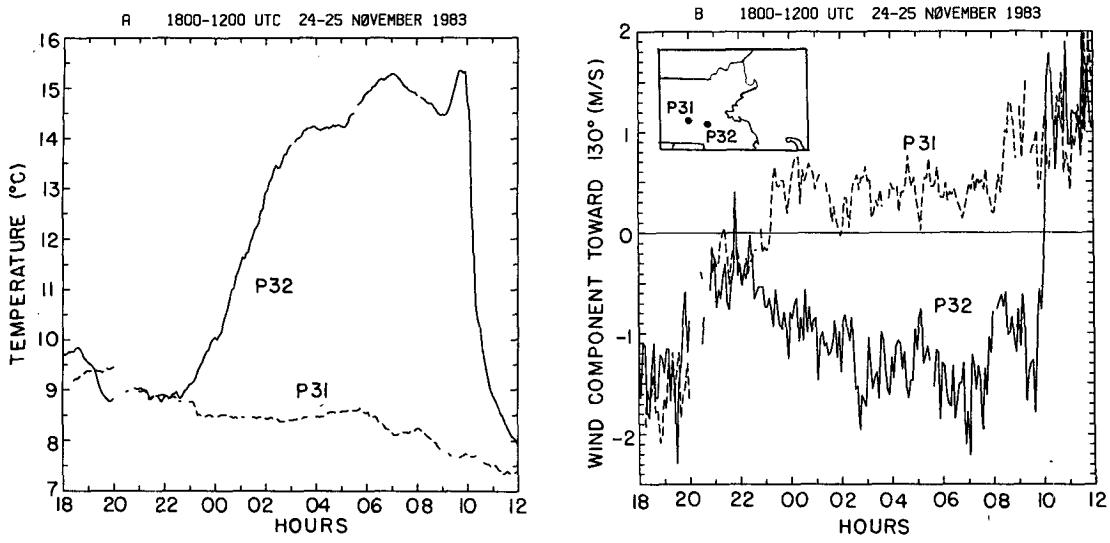

FIG. 15. Time series of (a) temperature and (b) front-normal wind speed (see text for definition) for PAM stations P31 and P32, 1800 UTC 24 Nov 1983 to 1200 UTC 25 Nov 1983.

al. 1945; Fisher 1960) have found well-developed sea breeze circulations with air temperature differences of 5°C, equivalent to a moderate Type A coastal front.

It appears from the two months of NEWSEX observations that heating of the air over water is a necessary element of both Type A and Type B coastal frontogenesis. Twice, onshore winds developed during NEWSEX in the absence of heating over water, but no coastal fronts developed. Despite light onshore winds, strong radiational cooling and coastal temperature differences of up to 8°C, no land breeze of significant geographical extent was able to develop along the southeastern New England coast. Nielsen (1987) gives a more complete discussion of these null events, including a case study.

Cooling of the air over land, while necessary by definition for Type B frontogenesis, may not be essential for Type A frontogenesis. By analogy with sea breezes, we expect that a large enough air–sea difference would produce a coastal front circulation in the absence of cooling over land. The evidence from NEWSEX, though, is inconclusive. No Type A fronts formed without diabatic cooling, but all daytime ridge passages occurred with air–sea temperature differences less than about 5°C.

Type A coastal fronts differ from ordinary land–sea breezes in that they are triggered by the veering of the ambient wind rather than by diurnal heating. Because the wind plays such a critical role in initiating Type A frontogenesis, we now examine the effect that ambient winds are known to have on ordinary sea breeze formation.

Opposing winds can prevent a sea breeze from occurring. Walsh (1974), in his linear model, found that the existence of a sea breeze depended on the inverse square of the opposing wind. Observational studies for

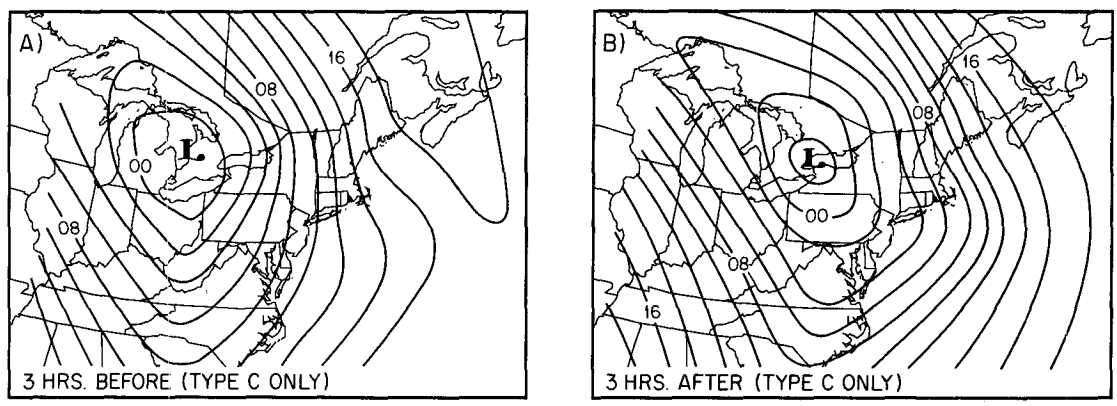

FIG. 16. Composite surface pressure analyses, as in Fig. 3, but for 4 Type C coastal front cases only.

the Great Lakes (Biggs and Graves 1962; Lyons 1972) have found a similar dependence. For those lake breezes, strong coastline-parallel winds were also inhibitory, probably because of the limited horizonal extent of the Great Lakes. However, if the opposing winds are not too strong to prohibit sea breeze formation, they serve to intensify the sea breeze front. Opposing winds in linear models produce stronger temperature gradients and vertical velocities (Walsh 1974), while following winds produce decreased temperature gradients and sea breeze winds (Ueda 1983). The generation or enhancement of sea breeze fronts by offshore winds has also been observed in the real atmosphere (e.g., Frizzola and Fisher 1963; Helmis et al. 1987) and simulated by numerical models (e.g., Pielke 1974). Estoque (1962) simulated the effect of both coastline-normal and coastline-parallel winds. The strongest front was associated with offshore winds, while onshore (following) winds weakened gradients considerably.

Based on these known characteristics of sea breezes, we may regard Type A coastal frontogenesis as taking place under conditions which are ideal for the development of an intense land–sea breeze front. With thermal forcing comparable to that associated with sea breezes, the initially very weak onshore winds favor the development of a robust solenoidal circulation. As the circulation intensifies, the increasing onshore winds favor rapid frontogenesis near the leading edge of the circulation.

Coastline-parallel winds, common during Type A frontogenesis, have less influence on sea breeze formation than coastline-normal winds. As Pearson et al. (1983) pointed out, coastline-parallel winds can have no effect at all in an inviscid sea breeze model with a straight, infinitely-long coastline. The two-dimensional numerical simulation by Estoque (1962) also found little influence by coastline-parallel winds. In the presence of a bay, coastline-parallel winds only modulate the sea breeze, intensifying it upstream and weakening it downstream (McPherson 1970). But the results of Roeloffzen et al. (1986) suggest that even in a two-dimensional model, coastline-parallel winds are conducive to front formation. Roeloffzen et al. (1986) have found that differential friction can cause a frontogenetical circulation to develop for an approximately ten degree range of geostrophic wind directions corresponding to northeasterly winds in New England. As geostrophic winds veer and become onshore, the front induced by friction would be located 15–20 km off the coast, but the theoretical position varies considerably with wind direction.

Because this induced frontal location is consistent with Type A frontogenesis observations, it is possible that frictional confluence helps to determine the location of Type A coastal frontogenesis. The Type B coastal front of section 3b may also have been assisted by frictional confluence. The early hypothesis that frictional deceleration of the onshore wind as it crosses the coast provides the necessary frontogenetical forcing for coastal front formation (Bosart 1975) is incorrect, however; as seen in the PAM observations, Type A frontogenesis occurs offshore well before the wind at the coastline has a chance to develop an onshore component.

b. A density current model of the effect of wind on developing coastal fronts

After formation, most Type A coastal fronts remain stationary or retreat with time, while sea breezes usually advance. A typical Type A coastal front will form just offshore, move slowly inland, and stall over land within 10 to 40 km of the coast. We now examine the hypothesis that this difference in behavior between coastal fronts and sea breezes is due to the interaction between the horizontal heating distribution and increasing onshore winds.

Pearson et al. (1983) attempted to specifically investigate the relationship between the speed of a sea breeze front and the opposing wind, and found a constant frontal speed relative to the opposing wind. However, Pearson et al. did not consider the effect of continuous thermal forcing. Two-dimensional models with a more realistic surface heating boundary condition, such as that of Kozo (1982), show that fronts tend to stall just onshore, with cross-shore velocities changing little in response to an increase in ambient wind speed.

The crucial factor in Kozo's simulation is the heating of the cold sea breeze as the air passes over the warm land surface. The farther inland a sea breeze penetrates, the warmer the cold air becomes before it reaches the front, and the smaller the frontal temperature difference. Fronts which are held closer to the coast by an opposing wind are able to remain more intense and can maintain a larger speed relative to the opposing wind.

Observations of sea and land breeze fronts have shown them to be density currents (Simpson 1969; Mitsumoto et al. 1983; Schoenberger 1984). The speed of a density current moving through a relatively lighter fluid is given by Benjamin (1968) as

$$C = u + K(gH\Delta\rho/\rho)^{1/2} \qquad (1)$$

where H is the depth of the density current, ρ is the density of the heavier fluid, $\Delta\rho$ is the density difference between the two fluids, and u is the velocity of the lighter fluid. In the atmosphere density is replaced by virtual potential temperature. The parameter K is of order 1 for atmospheric density currents. Neilley (1984) has made aircraft observations of two Type A New England coastal fronts 8 to 10 hours after formation. He found that both coastal fronts had the structure of density currents with values of K, using (1), of 1.03 and 1.11.

We have incorporated the density current equation (1) in a simple one-dimensional model in order to es-

timate the interaction of ambient wind and temperature on coastal front motion. The model assumes a straight coastline and a smoothly developing onshore wind. Boundary layer heat flux parameterizations are used to calculate the temperature of the air on either side of the front, given heating from the sea surface. Details of the model are contained in the Appendix.

Parameter values typical of New England coastal fronts (see Table A1) were used in the "control" model run. The air–sea temperature difference was taken to be 7.5°C. The warm-air wind speed was 7.5 m s^{-1}, with the wind veering gradually and becoming directly onshore after 10 hours. The results of the control run are shown in Fig. 17. Despite the smooth variation of the onshore wind and temperature, the modeled front changes direction twice and remains within 5 km of the coast for 16 hours. Initially the front moves offshore as the temperature difference rapidly grows along the front. As onshore winds intensify, the front is driven back across the coast at 7.9 hours, at which time the temperature difference across the front is 4.4°C. The specified onshore wind becomes steady after 10 hours, but the temperature difference continues to increase as warmer air reaches the front from offshore, and the front again moves offshore.

The apparently paradoxical situation of a quasi-stationary density current comes about because, even though the current is continuously accelerating into the opposing flow, the opposing flow is itself accelerating for the first 10 hours. If the two accelerations are nearly equal, as is the case in the control run, and the front is initially nearly stationary, the front will tend to remain *stationary relative to the ground.* In addition, fronts which manage to move offshore are slowed further by heating within the cold air from the sea surface.

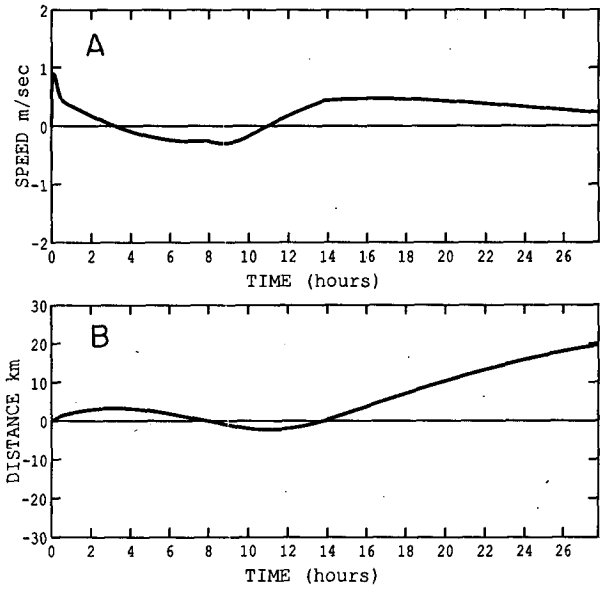

FIG. 17. (a) Speed (m s^{-1}, positive offshore) and (b) distance from coast (km, positive offshore) of density current versus elapsed time (hours), from control run of density current model described in text.

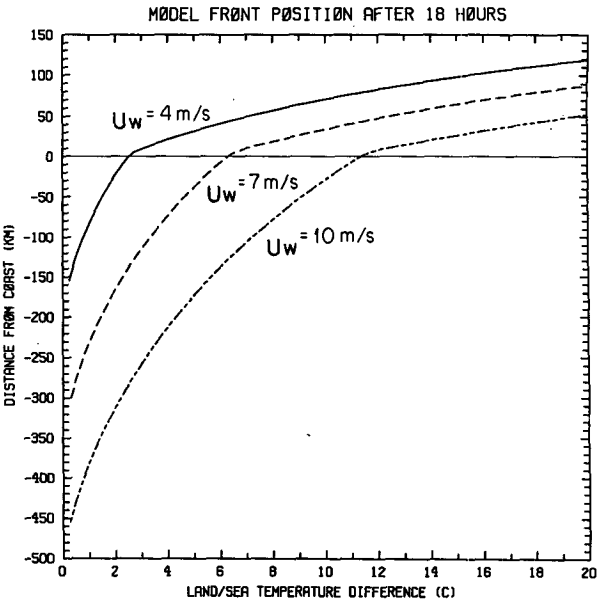

FIG. 18. Location (positive offshore) of coastal fronts after 18 hours, from density current model, as a function of temperature difference (°C) for warm air wind speeds of 4 m s^{-1}, 7 m s^{-1}, and 10 m s^{-1}.

The balance between wind and temperature may be directly altered by changing the magnitude of the air–sea temperature difference or the speed of the opposing wind. The position of the front relative to the coast after 18 hours is plotted in Fig. 18 for a range of temperature differences and three wind speeds encompassing conditions observed during NEWSEX. Other parameters are as in the control run. It can be seen that the stationary behavior of the control front is characteristic of a wide range of ambient wind and temperature conditions. Most modeled fronts remain close to the coastline, and roughly half are within 65 km of the coastline, implying an average frontal speed relative to the ground of less than 1 m s^{-1}. This quasi-stationary behavior of the fronts depends crucially on the effect of boundary-layer heating. If the heating is eliminated and the frontal temperature difference is a specified constant (a situation analogous to that considered by Pearson et al. 1983), the proportion of quasi-stationary fronts decreases by 80%.

Fronts which after 18 hours are more than 100 km inland generally have very weak temperature discontinuities (less than 2°C) and are almost entirely being advected by the onshore wind. Such weak, rapidly retreating fronts would be difficult to maintain in the presence of surface friction or orography. A modeled frontal location several hundred km inland may thus be regarded as a prediction by the model of no frontal formation at all.

Adjusting other free parameters of the model does not result in qualitative differences in the resulting fronts, and their effects are easily predictable. Decreasing the period of wind shift, for example, brings the front inland sooner, but does not change the eventual equilibrium position given by (A6). For the control model run, but with a complete wind shift after 5 rather than 10 hours, the front crosses the coast after only 2 hours and eventually penetrates 40 km inland before reversing direction after 12 hours. A wind shift over a period slightly longer than 10 hours keeps the front offshore throughout the integration. As for other parameters, increasing K or the cold air boundary-layer height increases the frontal speed relative to the warm air and produces frontal positions further east. Increasing the warm air boundary-layer height slows the heating and produces frontal positions further west. Increasing the heat flux parameters affects both sides of the fronts and causes them to remain closer to the coast.

As a test for a real coastal front case, the model was run with parameters appropriate to the 4 December 1983 coastal front case. The modeled front (not shown) remains near the coastline for 3 hours, and then moves inland in agreement with observations. After 7 hours, at the time the real front passes P24, the modeled front was about 13 km too far east and 2.2°C too strong. These differences are due to an overestimate of warm air temperatures, which can be attributed to the shape of the coastline. Because the real coastline swings eastward in Maine, air parcels are over water for less time than if the coastline were straight, as it is in the model. The lack of a variable air temperature over land also limits the usefulness of this version of the model for simulating actual cases.

Another deficiency of the model is the lack of topography. The mountain-parallel wind well inland from Type A and B coastal fronts is evidence of the influence of topography in channeling the cold air flow. The effect of cold-air damming on the coastal front is to accumulate the cold air against the mountains, which may result in an inverse relationship between frontal position and frontal height. This would produce an even greater tendency for coastal fronts to remain stationary, and may be the dominant influence on frontal motion after the cold dome has been established.

5. Cause of Type C coastal fronts

a. Theory and numerical modeling of upstream blocking by orography

The land–sea breeze mechanism does not account for type C coastal frontogenesis, which during NEWSEX took place away from the coast with the land–sea temperature differences being small or of the wrong sign with respect to the fronts. The other topographic feature in New England which can act to produce stationary fronts is the Appalachian mountain range. Interaction with topography is a common characteristic of long-lived coastal fronts of any type. New England coastal fronts have an oft-noted tendency to stall within a band stretching from Boston to Providence and extending roughly 20 km inland. Also associated with coastal fronts is the presence of an inverted ridge of high pressure between the front and the mountains caused by cold-air damming. The coastal front inversion has been found to form the upper margin of the dammed air in the Carolinas in cases studied by Bosart (1981) and Forbes et al. (1987).

The terms cold-air damming and upstream blocking refer to processes involving the flow of stratified fluid over orography. The relevant nondimensional parameter for such flows is the Froude number (Fr), which we shall define as

$$\mathrm{Fr} = NH/U, \tag{2}$$

where N is the Brunt-Väisälä frequency, H is the height of the orographic obstacle, and U is the wind speed normal to the obstacle. Laboratory, theoretical, and numerical studies (Baines and Hoinka 1985; Pierrehumbert 1984; Pierrehumbert and Wyman 1985) have indicated that blocking, or stagnation upstream of an obstacle, occurs in continuously stratified, deep, nonrotating fluids passing over a two-dimensional obstacle when Fr is greater than about two.

The addition of even a small amount of rotation, as discussed by Pierrehumbert and Wyman, prohibits the permanent blocking of inviscid, steady flows. The parameter which determines the importance of rotation is the local Rossby number

$$\mathrm{Ro} = U/fL \tag{3}$$

where L is the length scale of the windward mountain slope and U is the speed of the incident wind. For small Ro, semigeostrophic theory (Pierrehumbert 1985) predicts that the flow is never completely blocked, but a decelerated region does slope back from the mountain if Fr is sufficiently large.

The numerical simulations of Pierrehumbert and Wyman (1985) indicate that there is unsteady flow when $\mathrm{Ro} \geqslant 1$. It is in this parameter range that the orography of New England falls; taking 35 km as the length scale of the blocking mountain slope, onshore flows over the mountains of 5 to 15 m s^{-1} have Ro between 1.5 and 5.0. Although totally blocked fluid did develop in the simulations and persist for advective time scales of 1 to 6 (corresponding to a dimensional time of 3 to 5 hours for New England scales), it is not clear that blocked fluid would have formed if the fluid had been started from rest gradually rather than impulsively.

Garner (1986) recognized that the presence of warm advection in a rotating, stratified flow past orography could lead to enhanced blocking and frontogenesis. As such a flow is decelerated at low levels by the mountains, the orographically induced vertical shear in-

creases Fr by increasing the static stability in the shear region. This in turn feeds back to enhance the blocking. Because the flow far upstream of the mountain is unaffected, the temperature gradient perpendicular to the mountains leads to frontogenesis near the leading edge of the blocked region.

Garner used a two-dimensional model to determine the blocking characteristics of flows with $1 \leq \mathrm{Fr} \leq 1.5$ and $\mathrm{Ro} > 2$, a parameter range for which Pierrehumbert and Wyman predict no blocking. The parameter describing the advecting temperature gradient is, in Garner's notation, β, which for $\partial V/\partial x = 0$ is

$$\beta = \partial V/\partial z/N \qquad (4)$$

where V is the wind component in the y-direction (parallel to the mountain). Garner considered a north–south oriented mountain range with easterly flow U and southerly shear $\partial V/\partial z$ ($V = 0$ at $z = 0$). Here V is positive toward the south, so southerly shear implies negative β and warm advection.

The blocking criterion as a function of β, Fr, and Ro as calculated by Garner is shown in Fig. 19a. Garner's B5 mountain profile most closely resembles the orography of New England. The addition of warm advection via the β parameter causes blocking in the model for Fr near 1. For convenience, Fig. 19b shows the blocking criterion as a function of $\partial V/\partial z$, U, and $\partial\theta/\partial z$ for scales applicable to New England: $\theta_0 = 280$ K, $f = 1 \times 10^{-4}\ \mathrm{s}^{-1}$, $H = 500$ m, and $L = 35$ km. Garner's model with warm advection, unlike the theory and model of Pierrehumbert and Wyman with no warm advection, predicts total blocking of some upstream fluid for commonly observed winds and temperatures. The model also predicts frontogenesis at the leading edge of the blocked region. The addition of a north–south temperature gradient (a feature usually present during coastal frontogenesis) was found to enhance the circulation within the blocked air.

b. Comparison with observations

As described in section 3, the Type C coastal front of 25 November 1983 formed away from the seacoast, about two to four half-widths from the mountain ridge line, and moved slowly seaward. The frontogenesis occurred initially in Connecticut and propagated northward. The above theory, if applicable to this case, must account for the timing of frontogenesis as well as the change in onset time with position.

The values of the parameters β, Ro, and Fr (or, equivalently, U, $\partial V/\partial z$, and $\partial\theta/\partial z$) may be estimated from a sounding taken at PWM just prior to frontogenesis (Fig. 20). Steady rain was occurring at the time of the sounding, and the rain persisted through the

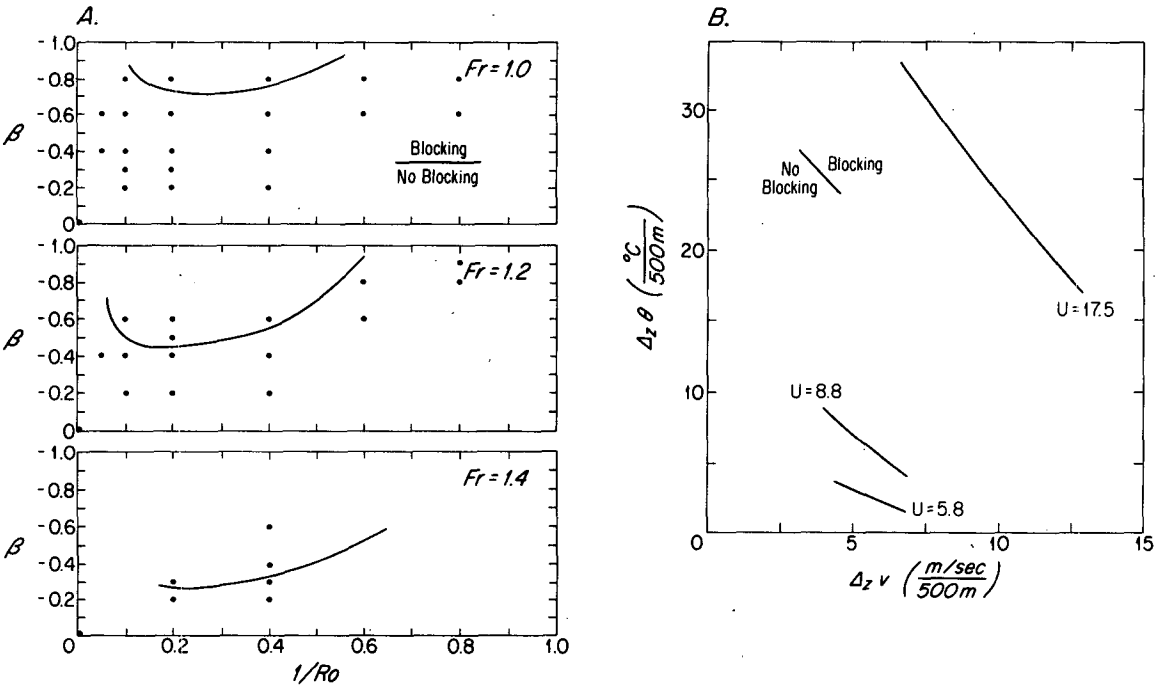

FIG. 19. (a) Blocking criteria as a function of 1/Ro, β, and Fr, as determined by numerical model runs for parameter values indicated by dots. Blocking occurs for values of parameters located above lines. The mountain profile used was an asymmetrical Gaussian with the lee slope five times as long as the windward slope. From Garner (1986). (b) Blocking criteria, as in (a), but as a function of mountain-normal wind speed and vertical gradients of potential temperature and mountain-parallel wind. Derived from Garner (1986) using external parameters appropriate to the topography of New England (see text). Vertical derivatives are normalized by the assumed height of the obstacle. Blocking occurs for values of parameters located above the lines.

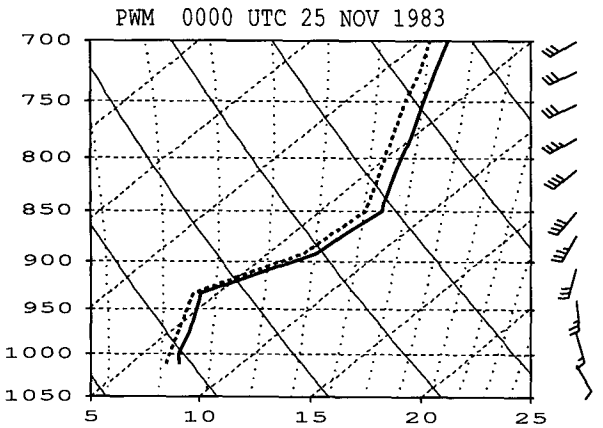

FIG. 20. Low-level skew-T diagram depicting temperature (solid) and dewpoint (dashed) in °C and winds (full barb equals 10 knots) for PWM, 0000 UTC 25 Nov 1983. Thin vertical background lines are constant potential temperature (solid), wet-bulb potential temperature (dotted), and temperature (dashed).

frontogenesis. The lowest atmospheric layer, nearly well-mixed in wet-bulb potential temperature, extended up to 930 mb (~700 m above ground level). It was capped by what appears to be a warm frontal inversion 80 mb thick, through which the temperature increased by 4°C. Above the inversion, the atmosphere was again nearly moist-adiabatic. The temperature structure at CHH (not shown) included a 30 mb thick inversion at the surface, overlain by a deep moist-adiabatic layer with properties similar to the upper layer at PWM. In addition, surface data (see Fig. 14) shows that the zone of strongest temperature gradient was progressing northward. It appears that at 0000 UTC 25 November 1983, an east–west baroclinic zone intersected the ground near southern Massachusetts and sloped upward toward the north, and that the baroclinic zone was moving slowly northward. This inference is corroborated by the PAM data; for example, the temperature at P32 (see Fig. 15a) increased 5°C in 4 hours during early evening. Similar temperature rises were observed at later times by PAM stations farther north.

To estimate the blocking characteristics at 0000 UTC, we divide the PWM sounding into three layers, the middle layer being the inversion. We orient our coordinate system so that U is positive toward 300 deg and V is positive toward 30 deg, parallel to the mountain. The vertical stratification is calculated using the wet bulb potential temperature. The calculated values of the blocking parameters are given in Table 2. The nearly neutral boundary layer is theoretically unblocked, but by inspection of Fig. 19b it may be seen that the inversion falls well above the blocking criterion for the mountain profile considered by Garner.

Frontogenesis, according to the theory, should have begun as the base of the inversion lowered toward the base of the mountains. As well as can be determined from the PAM data, this was indeed the case. Confluence was first noted at PAM stations at the same time as the initiation of the rapid temperature rises associated with the arrival of the baroclinic zone. This is seen in Fig. 15, in which steady confluence between P31 and P32 and the rapid temperature rise at P32 both commence at 2315 UTC. The observed northward propagation of coastal frontogenesis is accounted for by the south-to-north tilt and inferred lowering of the inversion at the surface baroclinic zone moved north. Thus, the coastal frontogenesis event of 25 November 1983 is well explained by the orographic frontogenesis model of Garner (1986).

Similar parameter calculations were made for the other three cases of Type C coastal frontogenesis during NEWSEX. As in the 25 November case, coastal frontogenesis occurred during the approach of warm frontal baroclinic zones, implying locally large values of $\partial V/\partial z$ and $\partial\theta/\partial z$. The case of 21 November 1983 involved blocking parameters similar to those of 25 November 1983. In the remaining two cases, parameters measured at PWM and CHH approached but did not exceed the blocking cutoff. However, large spatial variations make it difficult to estimate the temperature and wind structure in eastern Massachusetts and New Hampshire during those events, although in both cases there is evidence (from Doppler radar winds and additional soundings) that the forcing of Type C frontogenesis was stronger than could be estimated from the PWM and CHH soundings alone.

A final check of the theory is confirmation that it did not predict the formation of a coastal front when none occurred. Since it is unlikely that the blocking criterion is often satisfied outside warm frontal inversions, our check consisted of a search through NMC weather maps for all instances during NEWSEX of an analyzed warm front less than 300 km south of New England, with southerly to northeasterly winds to its north. All such warm fronts were found either to be associated with the remaining three Type C frontogenesis events (16 Nov, 20 Nov, 7 Dec) or to have approached New England while a Type A or Type B front was already present (11 Nov, 29 Nov, 22 Dec, 28 Dec).

6. Discussion

Using mesoscale NEWSEX data, we have identified three distinct processes of formation of New England coastal fronts, involving two dynamical mechanisms.

TABLE 2. Blocking parameters, PWM 0000 UTC 25 Nov 1983.

Layer (mb)	U (m s^{-1})	ΔV/500 m (m s^{-1})	$\Delta\theta_w$/500 m (°C)
1010–930	5.1	6.9	0.7
930–850	2.6	5.3	4.6
850–780	−6.2	−1.1	0.7

Type A and Type B coastal frontogenesis are a result of differential surface heating in the presence of a developing onshore airflow. A direct circulation, as robust as a sea breeze but in the direction of a land breeze, forms along the coastline, with the coastal front 10–20 km offshore. Type C coastal frontogenesis is consistent with upstream blocking of a stable, warm-advective airflow by a mountain range.

Type A and Type B frontogenesis are dynamically similar, the principal difference being a matter of timing. Type A frontogenesis occurs simultaneously with the initiation of onshore winds, with a land–sea temperature difference already present. Type B frontogenesis occurs during evening, as a land–sea temperature difference is established diurnally. Frictional confluence can aid both types of frontogenesis under suitable northeasterly flow conditions by concentrating the isotherms along the coast.

The phenomenon of warm frontal blocking, modeled by Garner (1986) and manifested during NEWSEX as Type C coastal frontogenesis, is a finite-width frontal zone analog to the conceptual model presented by Bjerknes and Solberg (1921):

> The warm front surface, which has usually a smaller inclination than that of the mountain slope, will reach the ridge and its passes while still a part of the cold air is lying below the slope. This cold mass will have no opportunity to escape as the way over the mountain ridge is already blocked by the overlying warm air. The lower part of the warm front surface will accordingly become stationary, supported by the mountains . . . (p. 21)

What Bjerknes and Solberg interpret as the lower part of the warm front surface is seen in our observations as a separate front, the Type C coastal front, which begins forming when the base of the warm frontal inversion impinges upon the mountains and is already well developed by the time the trailing edge of the warm front reaches it.

We have examined previous case studies of New England coastal fronts (excluding cases of "zipper lows") in an attempt to determine their type. It appears that all coastal fronts analyzed in detail by Bosart et al. (1972), Bosart (1975), Clark (1983), and Neilley (1984) were Type A coastal fronts, with the exception of what may have been a Type C coastal front on 4 December 1968 in Bosart et al. The abundance of Type A fronts may in part reflect the tendency of case studies to focus on the most extreme examples of the phenomenon under study.

A three-dimensional mesoscale numerical modeling study of New England coastal frontogenesis has been performed by Ballentine (1980). The initial conditions included a large air–sea temperature difference, but zero temperature gradient across the coastline. A temperature gradient soon formed, but the surface winds, initially northeasterly, had already veered onshore under the influence of an upper level trough. The resulting frontogenesis was a cross between Type A and Type B because, although the gradient formed like Type B in the presence of onshore winds, it was created entirely by heating. Ballentine found that heating and a veering onshore wind were of primary importance in forming the coastal front. When heating was suppressed, no coastal front formed. When veering was suppressed, the central portions of the coastal front moved offshore and were weaker, in agreement with the results of the density current model discussed in section 4. The motion of the modeled front is affected by lateral boundary conditions which force the front to remain stationary at the edges of the domain, so a direct comparison with density current frontal motions cannot be made.

It had been hoped that a clearer understanding of the mechanisms of coastal frontogenesis would facilitate the statement of a clear definition of coastal frontogenesis itself. This does not seem to be the case. A suitable definition may perhaps even exclude Type C frontogenesis, which is independent of the coastline. But a front delineating the margin of cold air trapped against mountains can be formed from Type A frontogenesis as well, and such a front need have no dependency on the coast, especially after warm advection has begun from the south.

Coastal fronts do not require the presence of mountains. Roeloffzen et al. (1986) noted the existence of coastal fronts forced by both differential heating and differential friction in the relatively flat Netherlands, and Ballentine (1980) found little change in the frontal circulations when the mountains were eliminated from his model. Nor do even Type A fronts depend on the presence of a coastline. Carolina coastal fronts apparently form 30–100 km offshore, along persistent heating discontinuities over water such as the west wall of the Gulf Stream (Riordan et al. 1985; SethuRaman and Riordan 1988). A catch-all definition, nevertheless excluding land breezes, seems appropriate:

> A coastal front is any front which forms parallel to and tends to remain quasi-stationary adjacent to a coastline, with warmer air seaward, and which forms as a result of upstream blocking or differential diabatic or frictional forcing, excluding those circulations driven solely by diurnal cooling (land breezes).

This definition intentionally excludes warm and cold fronts associated with classical cyclones. It also excludes "zipper low" fronts (Keshishian and Bosart 1987; Clark 1983) which are forced by geostrophic frontogenesis.

Because of the low density of operationally available surface data, coastal fronts may prove to be easier to forecast than to verify. With a large land–sea temperature difference, for example, a Type A coastal front can be expected to form along the coast as soon as winds veer onshore. An estimate of subsequent frontal motion might be made with a model such as the one discussed in section 4, but incorporating the geography

of New England. With lesser temperature differences and weak onshore winds, a Type B front would form in the evening if the initial onshore winds develop during midday. On the basis of the small number of NEWSEX cases and the composites in Fig. 16, Type C frontogenesis would be anticipated whenever a warm frontal inversion impinges upon the mountains. The four Type C fronts in NEWSEX all formed well inland, but the exact location of frontogenesis should depend upon the wind direction and the characteristics of the blocked airmass.

Acknowledgments. This research was partially supported by National Science Foundation Grants ATM82-09375 and ATM86-17132. I wish to thank Dr. Randall Dole, Dr. Kerry Emanuel, Peter Neilley, Joshua Wurman, and Christopher Davis for their support and criticism. The comments of the reviewers and editor helped to clarify several obscure aspects of the manuscript and give balance to competing frontogenetical mechanisms. The high quality of the PAM data set is due to the efforts of John Militzer and others associated with the PAM program at NCAR. The figures were drafted by Mike Rocha and Isabelle Kole.

APPENDIX

Description of the Density Current Model

Simpson et al. (1977) developed a density current model to investigate variations in the speed of an observed sea breeze. They specified the temperature of the warm air, the heating rate of the cold air, and the (constant) opposing warm air wind speed. Simpson et al. then integrated the density current equation (1) over time to determine the speed and location of the sea breeze front, and determined that a reduction of the speed of the front near midday was due to heating of the cold air. Here we apply a similar model to the coastal front problem to isolate the effects of wind and temperatures on coastal front motion. Unlike Simpson et al., we specify a time-dependent opposing wind and use a heat flux parameterization to calculate the temperature on both sides of the front.

The coastline is taken to be straight and infinitely long. It is oriented along the y axis with x positive in the offshore direction and zero at the coast. The coastal front is assumed to be a density current whose speed in the positive x direction is given by

$$C = u_w + K[gH_c(T_w - T_c)(T_W)^{-1}]^{1/2} \quad \text{(A1)}$$

where subscripts w and c refer to the warm and cold air, T is temperature, H is the height of the boundary layer or density current, g is gravity, K is the density current constant (see section 4b), and u is the x-component of the wind.[3]

[3] Simpson and Britter (1980, see their Fig. 3) have found a relationship between K and u_w. While it has often been inferred that their results imply that u_w should be multiplied by 0.62 in (A1), the relationship is not a linear one and for $u_w < 0$ (as is the case with coastal fronts), the multiplier approaches 1.

The veering wind associated with Type A coastal frontogenesis is represented as a constant warm air wind speed U_w and a wind direction which veers slowly from 270 deg at time $t = -L$ to 90 deg at time $t = L$. We assume well-mixed boundary layers with constant heights H_c and H_w, so that the thermodynamic equation for the warm and cold boundary layers becomes

$$dT/dt = 0, \qquad x < 0 \quad \text{(A2a)}$$

$$dT/dt = Q_{(z=0)}H^{-1}, \qquad x \geq 0 \quad \text{(A2b)}$$

in which surface heat fluxes are neglected over land and Q is the surface heat flux over water; Q is approximated from Eq. (27) of Deardorff (1972) as

$$Q = (A + BU)(T_s - T) \quad \text{(A3)}$$

with appropriate selection of the constants A and B. Here U is the total wind speed and T_s is the sea surface temperature.

Because U_w is constant, Eqs. (A2) and (A3) may be integrated over the total length of time a given warm air parcel is over water (t_s) to obtain an expression for its temperature:

$$T_w = T_s - (T_s - T_0)\exp\{H_w^{-1}(A + BU_w)t_s\} \quad \text{(A4)}$$

where T_0 is the initial air temperature (before air first crosses the coast). Because t_s is determined as a function of x and t by the specified warm air wind, (A4) determines the temperature of the warm air at any time and location. Because air which is farther offshore has been over water longer, (A4) implies a positive horizontal temperature gradient offshore.

For the cold air winds, the v component (v_c) is not predicted by density current theory. We assume it to be equal to the warm air v component. At later stages of frontal development, this underestimates the magnitude of v_c (see, for example, Fig. 5d), and results in a corresponding underestimate of the heating rate within the cold air when the front is over water. The front-normal wind component u_c is obtained from a relation which represents an average of laboratory and atmospheric data for density currents, from Simpson and Britter (1980, Fig. 4):

$$u_c = 1.2C - 0.2u_w. \quad \text{(A5)}$$

Using Eq. (A5), Eqs. (A2) and (A3) may be numerically integrated to obtain the cold air temperature at the front. An additional constraint, $u_c \geq u_0$, is needed when u_w is small to ensure a constant supply of cold air to the front, which in the real atmosphere would be provided by the induced direct circulation at the coast. Altering the value of u_0 has little effect except when $U_w < 3$ m s^{-1}.

The front is taken to be initially at the coastline ($x = 0$) at time $t = 0$. Successive positions of the front are obtained by stepping forward a time interval Δt, moving the front a distance $x = C/\Delta t$, calculating the new warm and cold air temperatures at the front, and using the prescribed winds to get the new coastal front

TABLE A1. Density current model parameters, control run.

A	0.004 m s^{-1}	Δt	10 s
B	0.015	T_0	270 K
H_c	300 m	T_s	277.5 K
H_w	1000 m	u_0	1.0 m s^{-1}
K	1.0	U_w	7.5 m s^{-1}

speed C. No starting temperature difference is imposed at the front, but a difference rapidly develops from the heating discontinuity and the front moves offshore during the first hour. It is the purpose of the model to accurately simulate not the initial frontal formation but the subsequent motion of the front, and simulated motions of the front during the first three hours or so should not be interpreted as being realistic.

If the model were to run indefinitely, the coastal front would approach a stationary position offshore at which the relative speed of the coastal front would be brought equal to that of the opposing wind by the heating of the cold air. This location, obtained from (A1)–(A5) and the specified warm air wind, is given by

$$X = H_c[B + A/\max(0.2U_w, u_0)] \times \ln\{K^2 g H_c (T_s - T_0)(T_s U_w^2)^{-1}\}. \quad \text{(A6)}$$

If the number in braces is less than 1 (that is, if the opposing wind is large relative to the temperature difference), no equilibrium position is possible and the front retreats from the coastline indefinitely.

The values of parameters used in the "control" model run are given in Table A1. The value of K has been selected as a simple compromise between coastal front values obtained by Neilley (1984) and sea breeze values obtained by Simpson (1969). Other values are representative of surface, rawinsonde, and aircraft observations of New England coastal fronts. For the control run, (A6) gives an asymptotic frontal position of 25.6 km.

REFERENCES

Baines, P. G., and K. P. Hoinka, 1985: Stratified flow over two-dimensional topography in fluid of infinite depth: a laboratory simulation. *J. Atmos. Sci.*, **42**, 1614–1630.

Ballentine, R. J., 1980: A numerical investigation of New England coastal frontogenesis. *Mon. Wea. Rev.*, **108**, 1479–1497.

——, 1982: Numerical simulation of land-breeze-induced snowbands along the western shore of Lake Michigan. *Mon. Wea. Rev.*, **110**, 1544–1553.

Bell, G. D., and L. F. Bosart, 1988: Appalachian cold-air damming. *Mon. Wea. Rev.*, **116**, 137–161.

Benjamin, T. B., 1968: Gravity currents and related phenomena. *J. Fluid Mech.*, **31**, 209–248.

Bergeron, T., 1949: The problem of artificial control of rainfall on the globe. Part II: The coastal orographic maxima of precipitation in autumn and winter. *Tellus*, **1**(3), 15–32.

Biggs, W. G., and M. E. Graves, 1962: A lake breeze index. *J. Appl. Meteor.*, **1**, 474–480.

Bjerknes, J., and H. Solberg, 1921: Meteorological conditions for the formation of rain. *Geofys. Publ.*, **2**(3), 60 pp.

Bosart, L. F., 1975: New England coastal frontogenesis. *Quart. J. Roy. Meteor. Soc.*, **101**, 957–978.

——, 1981: The Presidents' Day snowstorm of 18–19 February 1979: a subsynoptic-scale event. *Mon. Wea. Rev.*, **109**, 1542–1566.

——, 1984: The Texas coastal rainstorm of 17–21 September 1979: an example of synoptic-mesoscale interaction. *Mon. Wea. Rev.*, **112**, 1108–1133.

——, C. J. Vaudo and J. H. Helsdon, Jr., 1972: Coastal frontogenesis. *J. Appl. Meteor.*, **11**, 1236–1258.

Clark, D. A., 1983: A comparative study of coastal frontogenesis. M.S. thesis, Department of Meteorology, Massachusetts Institute of Technology, Cambridge, MA, 86 pp.

Craig, R. A., I. Katz and P. J. Harney, 1945: Sea breeze cross sections from psychrometric measurements. *Bull. Amer. Meteor. Soc.*, **26**, 405–410.

Deardorff, J. W., 1972: Parameterization of the planetary boundary layer for use in general circulation models. *Mon. Wea. Rev.*, **100**, 93–106.

Defant, F., 1951: Local winds. *Compendium of Meteorology*, T. F. Malone, Ed., Amer. Meteor. Soc., 655–672.

Draghici, I., 1984: Black Sea coastal frontogenesis. *Nowcasting II: Mesoscale Observations and Very-Short-Range Weather Forecasting*, European Space Agency, 75–79.

Estoque, M. A., 1962: The sea breeze as a function of the prevailing synoptic situation. *J. Atmos. Sci.*, **19**, 244–250.

Fisher, E. L., 1960: An observational study of the sea breeze. *J. Meteor.*, **17**, 645–660.

Forbes, G. S., R. A. Anthes and D. W. Thomson, 1987: Synoptic and mesoscale aspects of an Appalachian ice storm associated with cold-air damming. *Mon. Wea. Rev.*, **115**, 564–591.

Frizzola, J. A., and E. L. Fisher, 1963: A series of sea breeze observations in the New York City area. *J. Appl. Meteor.*, **2**, 722–739.

Garner, S. T., 1986: An orographic mechanism for rapid frontogenesis. Ph.D. thesis, Massachusetts Institute of Technology, Cambridge, MA, 222 pp.

Gross, G., 1986: A numerical study of the land and sea breeze including cloud formation. *Beitr. Phys. Atmos.*, **59**, 97–114.

Helmis, C. G., D. N. Asimakopoulos, G. D. Deligiorgi and D. P. Lalas, 1987: Observation of sea-breeze fronts near the shoreline. *Bound.-Layer Meteor.*, **38**, 395–410.

Keshishian, L. G., and L. F. Bosart, 1987: A case study of extended East Coast frontogenesis. *Mon. Wea. Rev.*, **115**, 100–117.

Kozo, T. L., 1982: A mathematical model of sea breezes along the Alaskan Beaufort Sea coast: Part II. *J. Appl. Meteor.*, **21**, 906–924.

Lyons, W. A., 1972: The climatology and prediction of the Chicago lake breeze. *J. Appl. Meteor.*, **11**, 1259–1270.

Mak, M. K., and J. E. Walsh, 1976: On the relative intensities of sea and land breezes. *J. Atmos. Sci.*, **33**, 242–251.

Marks, F. D., Jr., and P. M. Austin, 1979: Effects of the New England coastal front on the distribution of precipitation. *Mon. Wea. Rev.*, **107**, 53–67.

McPherson, R. D., 1970: A numerical study of the effect of a coastal irregularity on the sea breeze. *J. Appl. Meteor.*, **9**, 767–777.

Mitsumoto, S., H. Ueda and H. Ozoe, 1983: A laboratory experiment on the dynamics of the land and sea breeze. *J. Atmos. Sci.*, **40**, 1228–1240.

Neilley, P. P., 1984: Application of a density current model to aircraft observations of the New England coastal front. M.S. thesis, Department of Meteorology, Massachusetts Institute of Technology, Cambridge, MA, 64 pp.

Neumann, J., and Y. Mahrer, 1971: A theoretical study of the land and sea breeze circulation. *J. Atmos. Sci.*, **28**, 532–542.

Nielsen, J. W., 1987: The formation of New England coastal fronts. M.S. thesis, Department of Earth, Atmospheric, and Planetary Sciences, Massachusetts Institute of Technology, Cambridge, MA, 179 pp.

Niino, H., 1987: The linear theory of land and sea breeze circulation. *J. Meteor. Soc. Japan*, **65**, 901–921.

Passarelli, R. E., Jr., and R. R. Braham, Jr., 1981: The role of the winter land breeze in the formation of Great Lake snow storms. *Bull. Amer. Meteor. Soc.*, **62**, 482–491.

Pearson, R. A., G. Carboni and G. Brusasca, 1983: The sea breeze with mean flow. *Quart. J. Roy. Meteor. Soc.*, **109,** 809–830.

Pielke, R. A., 1974: A three-dimensional numerical model of the sea breezes over south Florida. *Mon. Wea. Rev.*, **102,** 115–139.

Pierrehumbert, R. T., 1984: Linear results on the barrier effects of mesoscale mountains. *J. Atmos. Sci.*, **41,** 1356–1367.

——, 1985: Stratified semigeostrophic flow over two-dimensional topography in an unbounded atmosphere. *J. Atmos. Sci.*, **42,** 523–526.

——, and B. Wyman, 1985: Upstream effects of mesoscale mountains. *J. Atmos. Sci.*, **42,** 977–1003.

Riordan, A. J., S. SethuRaman, J. M. Davis and S. Viessman, 1985: Measurements in the marine boundary layer near a coastal front. *Geophys. Res. Lett.*, **12,** 681–684.

Roeloffzen, J. C., W. D. Van Den Berg and J. Oerlemans, 1986: Frictional convergence at coastlines. *Tellus*, **38A,** 397–411.

Rotunno, R., 1983: On the linear theory of the land and sea breeze. *J. Atmos. Sci.*, **40,** 1999–2009.

Sanders, F., 1983: Observations of fronts. *Mesoscale Meteorology—Theories, Obervations, and Methods*, D. K. Lilly and T. Gal-Chen, Eds., D. Reidel, 175–203.

Schoenberger, L. M., 1984: Doppler radar observations of a land-breeze cold front. Mon. Wea. Rev., **112,** 2455–2464.

Sethu Raman and A. J. Riordan, 1988: The Genesis of Atlantic Lows Experiment: The planetary-boundary-layer subprogram of GALE. *Bull. Amer. Meteor. Soc.*, **69,** 161–172.

Simpson, J. E., 1969: A comparison between laboratory and atmospheric density currents. *Quart. J. Roy. Meteor. Soc.*, **95,** 758–765.

——, and R. E. Britter, 1980: A laboratory model of an atmospheric mesofront. *Quart. J. Roy. Meteor. Soc.*, **106,** 485–500.

——, D. A. Mansfield and J. R. Milford, 1977: Inland penetration of sea-breeze fronts. *Quart. J. Roy. Meteor. Soc.*, **103,** 47–76.

Ueda, H., 1983: Effects of external parameters on the flow field in the coastal region—a linear model. *J. Climate Appl. Meteor.*, **22,** 312–321.

Walsh, J. E., 1974: Sea breeze theory and applications. *J. Atmos. Sci.*, **31,** 2012–2026.

Watts, A. J., 1955: Sea-breeze at Thorney Island. *Meteor. Mag.*, **84,** 42–48.